Universidade do Estado do Rio de Janeiro

Centro de Tecnologia e Ciências

Faculdade de Engenharia

Manuchi Martins Dansa

Sliding Mode Control for Classes of Nonlinear Biological and Chaotic Systems with Uncertainties

Rio de Janeiro

2019

Manuchi Martins Dansa

Sliding Mode Control for Classes of Nonlinear Biological and Chaotic Systems with Uncertainties

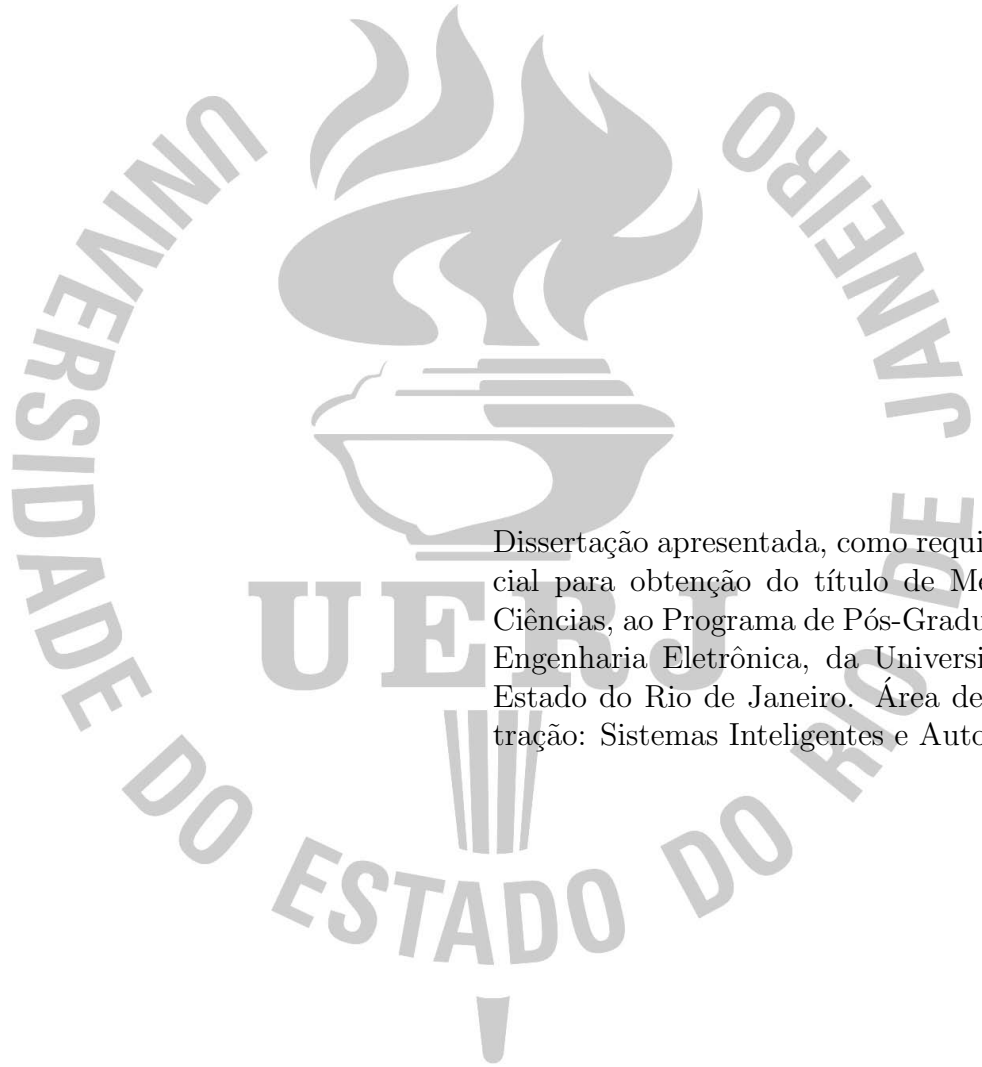

Dissertação apresentada, como requisito parcial para obtenção do título de Mestre em Ciências, ao Programa de Pós-Graduação em Engenharia Eletrônica, da Universidade do Estado do Rio de Janeiro. Área de concentração: Sistemas Inteligentes e Automação.

Orientador: Prof. Dr. Tiago Roux de Oliveira

Rio de Janeiro

2019

CATALOGAÇÃO NA FONTE

UERJ / REDE SIRIUS / BIBLIOTECA CTC/B

D191 Dansa, Manuchi Martins.
Sliding mode control for classes of nonlinear biological and chaotic systems with uncertainties / Manuchi Martins Dansa. – 2019.
80f.

Orientador: Tiago Roux de Oliveira.
Dissertação (Mestrado) - Universidade do Estado do Rio de Janeiro, Faculdade de Engenharia.

1. Engenharia eletrônica - Teses. 2. Sistemas de controle por realimentação - Teses. 3. Sistemas não-lineares - Teses. I. Oliveira, Tiago Roux de. II. Universidade do Estado do Rio de Janeiro. III. Título.

CDU 681.511.4

Bibliotecário: Iremar Leal da Silva CRB7/5728

_____ _____

Assinatura Data

Manuchi Martins Dansa

Sliding Mode Control for Classes of Nonlinear Biological and Chaotic Systems with Uncertainties

Dissertação apresentada, como requisito parcial para obtenção do título de Mestre em Ciências, ao Programa de Pós-Graduação em Engenharia Eletrônica, da Universidade do Estado do Rio de Janeiro. Área de concentração: Sistemas Inteligentes e Automação.

Aprovado em 30 de julho de 2019.
Banca Examinadora:

Prof. Dr. Tiago Roux de Oliveira, D.Sc. (Orientador)
Faculdade de Engenharia - UERJ

José Paulo Vilela Soares da Cunha, D.Sc.
Faculdade de Engenharia - UERJ

Prof. Dr. Andrei Giordano Holanda Battistel, D. Sc.
Faculdade de Engenharia - UERJ

Prof. Dr. Americo Barbosa da Cunha Junior, D.Sc.
Instituto de Matemática e Estatística - UERJ

Prof. Dr. Antonio Candea Leite, D. Sc.
Departamento de Engenharia Elétrica - PUC-Rio

Rio de Janeiro
2019

DEDICATÓRIA

Dedico este trabalho aos meus pais.

AGRADECIMENTO

Agradeço aos meus amigos e familiares. Agradeço também ao meu orientador Tiago Roux de Oliveira e ao amigo Victor Hugo Pereira Rodrigues pelas orientações que me deram e que foram de fundamental importância à conclusão desta dissertação. Por fim, volto um agradecimento especial aos professores José Paulo Vilela Soares da Cunha, Andrei Giordano Holanda Battistel, Americo Barbosa da Cunha Junior e Antonio Candea Leite por terem aceitado o convite de participação da banca examinadora. Suas recomendações e orientações foram de grande valia para o aperfeiçoamento deste trabalho que o leitor tem agora em mãos.

RESUMO

DANSA, Manuchi Martins. *Sliding Mode Control for a Class of Nonlinear Biological and Chaotic Systems with Uncertainties*. 80 f. Dissertação (Mestrado em Engenharia Eletrônica) - Faculdade de Engenharia, Universidade do Estado do Rio de Janeiro (UERJ), Rio de Janeiro, 2019.

Nessa dissertação, são propostas estratégias de controle que sejam capazes de estabilizar sistemas incertos, não lineares, monovariáveis, e de grau relativo arbitrário utilizando apenas realimentação de saída. Em especial, deseja-se alcançar a estabilização local ou global de duas classes de sistemas: os sistemas feedforward-like e os sistemas strict-feedback. Para lidar com o problema de incertezas da planta, as leis de controle adotadas serão baseadas no controle robusto por modos deslizantes, tenham elas uma natureza contínua ou chaveada. Além disso, para compensar o grau relativo excedente, é necessário projetar uma variável de deslizamento que seja descrita a partir de uma combinação linear da saída e de suas derivadas. Nesse contexto, surge a necessidade de se utilizar um diferenciador robusto e exato, baseado em modos deslizantes de ordem superior e de ganho fixo. Sendo este ganho dependente do vetor de estado da planta, o uso de observadores da norma em cascata se faz necessário para estimar a parcela desconhecida do estado. Tal estimativa pode ser feita a partir do conhecimento de limitantes superiores e inferiores dos parâmetros incertos do sistema. Desse modo, explorando propriedades ISS (Input-to-State Stable/Stability) dos sistemas em estudo, é possível garantir que os controladores propostos são capazes de estabilizar globalmente ou de regular localmente os sistemas considerados. Sistemas caóticos e biológicos são tomados como aplicações dos algoritmos propostos. Quanto aos sistemas caóticos, é proposto um esquema de comunicação segura a partir da sincronização de osciladores caóticos de um sistema mestre-escravo. No que diz respeito aos sistemas biológicos, deseja-se regular a glicemia em pacientes diabéticos Tipo 1.

Palavras-chave: Controle por Modos Deslizantes; Realimentação de Saída; Estabilidade Entrada-Estado; Sistemas Feedforward-like; Sistemas Strict-feedback.

ABSTRACT

DANSA, Manuchi Martins. *Sliding Mode Control for a Class of Nonlinear Biological and Chaotic Systems with Uncertainties.* 80 f. Dissertation (Master Degree Course in Electronic Engineering) - Faculdade de Engenharia, Rio de Janeiro State University (UERJ), Rio de Janeiro, 2019.

In this dissertation, control strategies are proposed in order to stabilize uncertain, nonlinear and monovariable systems of arbitrary relative degree in such a way that only output feedback is used. In particular, it is desired to achieve local or global stabilization of two classes of systems: feedforward-like systems and strict-feedback systems. To deal with the plant uncertainty problem, the control laws adopted will be based on robust control by sliding modes, whether these are continuous or switched in nature. In addition, to compensate for the relative excess degree, it is necessary to design a sliding variable that is described from a linear combination of the output and its derivatives. In this context, the need arises to use a robust and exact differentiator, based on sliding modes of higher order and fixed gain. Since this gain depends on the state vector of the plant, the use of observers of the cascade norm is necessary to estimate the unknown portion of the state. Such an estimate can be made from knowledge of upper and lower limiting uncertain system parameters. Thus, by exploiting ISS (Input-to-State Stable / Stability) properties of the systems under study, it is possible to guarantee that the proposed controllers are able to stabilize globally or to regulate locally the considered systems. Chaotic and biological systems are taken as applications of the proposed algorithms. As for chaotic systems, a secure communication scheme is proposed by using the synchronization of chaotic oscillators of a master-slave system. With regard to biological systems, it is desired to regulate blood glucose in Type 1 diabetic patients.

Keywords: Sliding Mode Control; Output Feedback; Input-State Stability; Feedforward-like systems; Strict-feedback systems.

LIST OF FIGURES

LIST OF TABLES

SUMMARY

INTRODUCTION[1]

In the world of recursive control designs for nonlinear systems, two basic classes of systems are the most easily recognizable - the systems with (strict-)feed*back* structure and the systems with (strict-)feed*forward* structure. The strict-feedback systems, which occupied the attention of the nonlinear control community in the first half of the 1990's, are controlled using *backstepping*, a method that employs aggressive controls[2] necessary to suppress finite escape instabilities inherent (in open loop) to strict-feedback systems. In contrast, the strict-feedforward systems, which were studied intensively in the mid- and late-1990's, can be only marginally unstable in open loop,[3] and permit (and in many cases call for) cautious controllers.

The theoretical foundation of how to exercise 'caution' in the design for feedforward systems was laid by Teel in his 1992 dissertation [3], where he introduced the technique of nested saturations whose parameters are carefully selected to essentially achieve robustness of linear controllers to nonlinearities (of superlinear and other types). Soon after this first design, Teel [4] developed a series of results that, among other things, interpreted and generalized [3] in the light of nonlinear small gain techniques that he developed in [4].

The next major spurt of progress came with the paper of Mazenc and Praly [5], which introduced a Lyapunov approach for stabilization of feedforward systems. This approach, initially conceived in March 1993, has its roots that go further back to Praly's designs for adaptive nonlinear control [6] and output feedback stabilization [7] where he was designing forwarding like coordinate changes involving a stable manifold that can be written as a graph of a function. A related idea was used by Sontag and Sussmann [8] for stabilization of linear systems with saturated controls. Recently, Praly, Ortega, and Kaliora [9] relaxed the conditions under which such manifolds can be found.

Jankovic, Sepulchre, and Kokotovic [10] developed a different Lyapunov solution to the problem of forwarding (and stabilization on a broad class of cascade systems), which, rather than a coordinate change or domination of (certain) 'cross terms' (as Mazenc and Praly), employs an exact cross term in the Lyapunov function. In [11] they presented an algorithmic, inverse optimal design for a class of feedforward systems and provided a detailed insight into the structure of the target system in the forwarding recursion.

---

[1] This introduction was originally written by Krstic in [2].

[2] As measured by growth of their nonlinearities

[3] With solutions growing only polyomially in time

Further developments of feedorward systems have gone in several directions. The nested saturation ideas have been expanded upon Arcak, Teel, and Kokotovic [12], Marconi and Isidori [13], and Xudong [14]. Implicit (or explicit) in the first three papers are robustness results with respect to certain classes of unmodeled dynamics. The Lyapunov approach has been developed further by Sepulchre, Jankovic, and Kokotovic [11], [15], Mazenc, Sepulchre, and Jankovic [16] and Mazenc and Praly [17]. In [18] Teel designed $\mathscr{L}_2$ stabilizing controllers for feedforward systems ($\mathscr{L}_\infty$ disturbance attenuation, while impossible in general, remains a problem of interest for subclasses of feedforward systems). Trajectory tracking, while hard to achieve for arbitrary trajectories, has been solved under reasonable conditions by Mazenc and Praly [19] and Mazenc and Bowong [20]. Extensions to nonlinear integrator chains have been proposed by Mazenc [21] and Tsinias and Tzamtzi [22]. Even a generalization to feedforward systems with exponentially unstable linearizations has been reported by Grognard, Sepulchre, and Bastin [23]. Discrete time feedforward systems have also been studied, in a recent paper by Mazenc and Nijmeijer [24]. Linear low-gain semi-global stabilization of feedforward systems was proposed by Grognard, Basin, Sepulchre, and Praly [25]. Differential geometric characterization of feedforward systems has eluded researchers until recent major progress was reported by Tall and Respondek [26]. Starting with Teel's original interest in the ball-and-beam problem [3] and Mazenc and Praly's design for the pendulum-cart problem [5], the research on forwarding has continuously been driven by applications. The following papers on forwarding are fully (or almost fully) dedicated to applications: Spong and Praly [27] (pole-cart), Barbu, Sepulchre, Lin, and Kokotovic [28] (ball-and-beam), Albouy and Praly [29] (spherical inverted pendulum), Praly, Ortega,and Kaliora [9] (inverted pendulum with disk inertia), and Mazenc and Bowong [30] (pendulum-cart), and Praly [31] (satellite orbit transfer with weak but continuous thrust). For tutorial coverage of forwarding, the reader is referred to the book of Sepulchre, Jankovic, and Kokotovic [15] and to Praly's tutorial [31] (available from his web page). Some coverage of forwarding is also available in the surveys by Coron, Praly, and Teel [32] and Kokotovic and Arcak [33].

In this dissertation, we desire to discuss how, in particular, the nonlinear sliding mode controller can be applied in these classes of systems: strict-feedback systems and feedforward-like systems, presenting advantages and restrictions.

Feedforward-like Systems

We consider the control of nonlinear systems in so-called "feedforward-like" form.

$$\dot{x}_1 = a_1 x_1 + \phi_1(x_2, x_3, x_4, x_5, \ldots, x_{n-1}, y, t)\,, \tag{1}$$

$$\dot{x}_2 = a_2 x_2 + \phi_2(x_3, x_4, x_5, \ldots, x_{n-1}, y, t)\,, \tag{2}$$

$$\dot{x}_3 = a_3 x_3 + \phi_3(x_4, x_5, \ldots, x_{n-1}, y, t)\,, \tag{3}$$

$$\dot{x}_4 = a_4 x_4 + \phi_4(x_5, \ldots, x_{n-1}, y, t)\,, \tag{4}$$

$$\vdots \tag{5}$$

$$\dot{x}_{n-1} = a_{n-1} x_{n-1} + \phi_{n-1}(y, t)\,, \tag{6}$$

$$\dot{x}_n = \phi_n(x_1, x_2, x_3, x_4, x_5, \ldots, x_{n-1}, y, t) + k_p u\,, \tag{7}$$

$$y = x_n\,, \tag{8}$$

with $a_i \in \mathbb{R}$ being scalar, $x_i \in \mathbb{R}$, for $i = 1, \ldots, p-1$, are the state variables of the system, $u \in \mathbb{R}$ is the control input, y is the output signal, $k_p \in \mathbb{R}$ is the control gain and where the functions $\phi_i(\cdot)$ are $n-1$ times differentiable. The objective is to design a controller that stabilizes the state vector $X := [x_1, x_2, \ldots, x_n]^T$.

In particular, biological and chaotic systems belong to this classes of systems.

Strict-Feedback Systems

We consider the control of nonlinear systems in so-called "strict-feedback" form.

$$\dot{x}_1 = a_1 x_2 + \phi_1(x_1, t)\,, \tag{9}$$

$$\dot{x}_2 = a_2 x_3 + \phi_2(x_1, x_2, t)\,, \tag{10}$$

$$\dot{x}_3 = a_3 x_4 + \phi_3(x_1, x_2, x_3, t)\,, \tag{11}$$

$$\dot{x}_4 = a_4 x_5 + \phi_4(x_1, x_2, x_3, x_4, t)\,, \tag{12}$$

$$\vdots \tag{13}$$

$$\dot{x}_{n-1} = a_{n-1} x_n + \phi_{n-1}(x_1, x_2, x_3, x_4, \ldots, x_{n-1}, t)\,, \tag{14}$$

$$\dot{x}_n = \phi_n(x_1, x_2, x_3, x_4, \ldots, x_n, t) + k_p u\,, \tag{15}$$

with $a_i \in \mathbb{R}$ being scalar, $x_i \in \mathbb{R}$ being the state variables of the system, $u \in \mathbb{R}$ is the input, $k_p \in \mathbb{R}$ is the control gain and where each function $\phi_i(\cdot)$ is a function of class C^{n-1}. The relative degree of system (1)–(15) determines who is its output. Since we desire to represent a "strict-feedback" system with a generic relative degree, the output is not defined *a priori*.

Sliding Mode Control

Sliding mode control is a well documented technique, and its fundaments might be found in [34] and [35]. In this section, the major features of this technique are revisited.

In order to design a classic sliding mode controller, we must follow a procedure composed by two steps. The first one consists in the design of the ideal sliding variable, σ, with unitary relative degree, ρ, with respect to the discontinuous control law, $u(t)$. It means that the control law must appear explicitly in $\dot{\sigma}$. The second step consists in the design of a control law that can be able to guarantee that the system enters in *sliding mode* in finite time.

The system enters in sliding mode at the instant where the sliding variable reaches the sliding surface ($\sigma = 0$)[4]. Once in sliding mode, the system becomes insensible to limit and matched disturbances; and, beyond that, the original system normally assumes a novel representation, a representation of a system of reduced order. This new system will be referenced here by *sliding mode dynamics*.

At the initial stage of the design, we must predict the sliding mode dynamics, and then design the sliding variable with the goal of stabilizing it. In such a way, it is worth remarking that the sliding variable converges to the sliding surface in finite time. However, the sliding mode dynamics is normally stabilized asymptotically.

The major disadvantage of the classic sliding mode is the phenomenon known as *chattering*. This phenomenon is characterized by small oscillations at the system output and may impair the performance of control systems. The chattering effect can arise due to high frequency nonmodeled dynamics, or due to problems related to digital implementation. Nevertheless, the chattering effect can be mitigated by the implementation of different techniques of which *Boundary Layer* [37] is an example.

In this dissertation, the author aims to investigate the application of such control strategy to feedforward-like systems.

[4]In another words, the so called *sliding surface* represents the geometric place or the locus of points where $\sigma = 0$, inside the state space [36].

Organization of the Text

This dissertation is organized as follows. Chapter 1 has as its main objective to propose control algorithms that ensure the regulation of blood glucose in type 1 diabetic patients. In healthy people, blood glucose is primarily regulated by two hormones, insulin and glucagon, both secreted by the pancreas and with opposite actions. While insulin is responsible for facilitating the transfusion of the glucose from the blood flow to the cells, decreasing blood glucose levels, glucagon acts in order to increase the concentration of glucose in the blood. On the other hand, in subjects with type 1 Diabetes Mellitus (T1DM), the normal blood glucose regulation is impaired. In this context, control algorithms for a bihormonal artificial pancreas are proposed in such a way that insulin and glucagon actions are incorporated, aiming to avoid hiperglycemic and hypoglycemic cases – the latter usually found in single insulin-based approaches. Although, the mathematical model utilized has experimental validation and represents satisfactorily the glucose-insulin-glucagon dynamics, it contains parametric uncertainties and unmatched disturbances due to food intake which are compensated by sliding mode control algorithms through a bihormonal pump (insulin plus glucagon). Two different control strategies are employed: First-Order Sliding Mode as well as Terminal Sliding Mode Controllers (in their continuous and discontinuous versions). A rigorous stability analysis is carried out for both closed-loop systems by means of Lyapunov's theory. The stability proof is presented assuming that the state is known. However, exact differentiators are used in the simulation results to recover the information associated with the state variables of the system, which in a realistic scenario are assumed to be unmeasured.

Next, in Chapter 2, we have assumed that the parameters of a seven-dimensional hyperchaotic system are uncertain and only the output variables are available for feedback (partial-state feedback). Exploring ISS (Input-to-State Stability) properties of the system, an upper bound for the norm of the unmeasured state vector is developed from the system outputs. Such a norm estimate provided by cascade norm observers is applied to obtain the output-feedback sliding mode control law. Based on Lyapunov's stability theory, it was possible to guarantee that the proposed controller is able to globally stabilize the considered hyperchaotic system, i.e., the initial conditions can be arbitrary.

Objectives

As discussed earlier, in this thesis, control strategies are proposed in order to stabilize uncertain, nonlinear and monovariable systems of arbitrary relative degree in such a way that only output feedback is used. In particular, it is desired to achieve local or global stabilization of feedforward-like systems. Chaotic and biological systems are taken as applications of the proposed algorithms.

Concerning chaotic systems, a secure communication scheme is proposed by using the synchronization of chaotic oscillators of a master-slave system. With regard to biological systems, it is desired to regulate blood glucose in Type 1 diabetic patients.

Moreover, it is noteworthy that the case addressed in this thesis encompasses the presence of parametric uncertainties, exogenous disturbances and nonlinearities of the plant. In this sense, the control strategies adopted stand out for the following advantages:

- Robustness to parametric uncertainties ;
- Robustness to exogenous disturbances ;
- Robustness to nonlinearities of the plant ;
- Control objective reached in finite time .

This concludes the introductory discussions of the thesis.

1 BLOOD GLUCOSE REGULATION IN PATIENTS WITH TYPE 1 DIABETES BY MEANS OF OUTPUT-FEEDBACK SLIDING MODE CONTROL

1.1 Introduction

The pancreas, in addition to its digestive functions, secretes two important hormones, *insulin* and *glucagon*, that are crucial for normal regulation of blood glucose concentration [38]. When the glucose concentration rises above a certain level, insulin is secreted; the insulin in turn causes the blood glucose concentration to drop toward normal. Conversely, a decrease in blood glucose stimulates glucagon secretion; the glucagon then functions in the opposite direction to increase and then steer the glucose back to its normal level.

However, in patients with type 1 Diabetes Mellitus (T1DM), pancreatic insulin production is impaired, which entails a plenty of risks to these patients health. Tight glucose control reduces the risk of long-term diabetes related complications, such as kidney disease, heart disease, blindness and peripheral vascular and nerve damage. Moreover, conventional methods of self-monitoring of blood glucose and multiple daily injections are challenging for patients and families [39].

Against such a background, an automated closed-loop glucose control system stands out as a target that has been pursued by researchers for the past five decades [40]. Such devices, known as artificial pancreas [41], [42], consist of a glucose sensor, from which data are collected and entered into an algorithm, which in turn compute the amount of insulin to be delivered through a pump. Figure 1 depicts how such a device could be.

1.1.1 Motivation

In modeling drug delivery to human body, certain requirements like finite reaching time and robustness to uncertainties, should be satisfied [44]. In addition, the glucose-insulin dynamics is a complex physiologic system that encompass a number of nonlinear process and therefore cannot be accurately described through linear models [45].

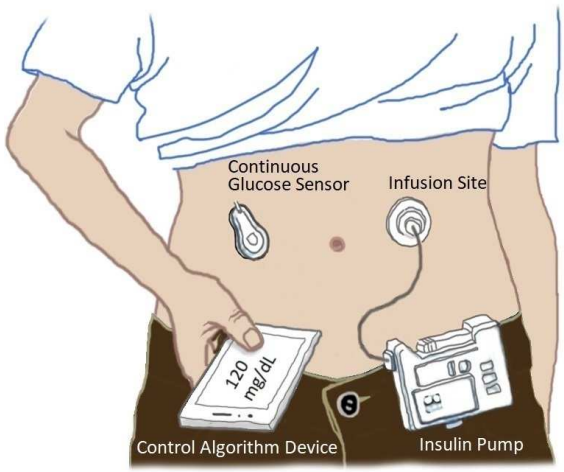

Figure 1: Mono-hormonal artificial pancreas. A bihormonal artificial pancreas should yet add a pump for the hormone glucagon. Illustration made by Salmo Dansa and adapted from: [43] [Accessed: 29 April 2019]

As discussed in the following, it is noteworthy that a plenty of different control strategies could have been used in order to assure the maintenance of normal glucose concentrations (euglycemia).

1.1.2 State-of-the-Art of the Control Algorithms for Blood Glucose Regulation

The most commonly used controllers are based on proportional-integral-derivative control (PID) [46], [47], [48], model predictive control (MPC) [49], [50], [51], [52], adaptive control [53], [54], [55], fuzzy logic control and artificial neural network approach [56].

Sliding Mode Control has been proved an efficient technique to provide high-fidelity performance in different control problems for nonlinear systems with uncertainties in system parameters and external disturbances [57].

In particular, one alternative approach and control technique that has been tested for closed-loop control of blood glucose is the fast terminal sliding mode controller (FTSMC) [58]. Although this controller seems to be more robust to uncertainties in the model and presents faster responses when compared to the references above, the full-state measurement is required and no stability proof was carried out for the closed-loop system.

1.1.3 Dual-Hormone Strategy

Concerning the pump actuator for drug delivery, there is a question that has generated much controversy in the artificial pancreas community: to utilize single-hormone

systems employing only insulin or to adopt a dual-hormone strategy adding glucagon administration to insulin delivery. Although insulin-only closed-loop systems achieve a much better glycemic control than standard open-loop insulin therapy, it does not completely eliminate the risk of hypoglycemia [39], [59], [60].

On the other hand, a closed-loop system that employs subcutaneous infusion of both insulin and glucagon has proven its efficacy in preventing and treating hypoglycemia [61], [62]. Moreover, such bihormonal systems would better emulate the function of the endocrine pancreas [63] and, for this reason, will be considered in this chapter.

Pumps used for diabetic patients infuse hormone subcutaneously. In this sense, *in silico* testing of a dual-hormone control algorithm requires a suitable model that is able to simulate the effects of subcutaneously administered insulin and glucagon [64]. In this essay, we implement the model proposed by [65] extended with glucagon action as proposed by [66].

1.1.4 Contributions

The purpose of this contribution is to introduce closed-loop sliding mode control algorithms capable of regulating the blood glucose concentration in subjects with T1DM through a bihormonal pump. A rigorous stability analysis is carried out by means of Lyapunov's theory taking into account parametric uncertainties in the biological model and unmatched disturbances due to food intake. Two different control strategies are proposed: First-order Sliding Mode Control (FOSMC) and Non-Singular Terminal Sliding Mode Controller (NSTSMC). Continuous versions of the algorithms are also addressed.

Numerical simulations illustrate the efficiency of both control strategies. The output-feedback version of the proposed algorithms using higher-order sliding mode (HOSM) differentiators is also discussed and evaluated.

1.1.5 Chapter Outline

All things considered, it should be said that this chapter is organized as follows. In Section 1.3, the mathematical model used in this manuscript is exposed. The methodology and the control objectives are the themes of Section 1.4. In 1.5, we discuss how food intake is handled as an unmatched disturbance of the system dynamics. Section 1.6 presents the bihormonal actuator description and the physical interpretation of the two

control actions of the controller. The subsequent two sections deal with the sliding mode control algorithms applied to achieve the control goals. Section 1.7 shows the First Order Sliding Mode Control (FOSMC); while Section 1.8 introduces the Fast Terminal Sliding Mode Control (FTSMC). Next, an exact differentiator based on Higher-Order Sliding Modes (HOSM) is properly discussed in Section 1.9. At last, Section 1.10 presents some numerical examples.

1.2 Compartmental Systems

Compartmental systems are frequently utilized for being conceptually simple and, even though, quite efficient in the description of phenomenological features considered essentials in dynamic systems. Compartmental systems are ruled by conservative laws and are composed by homogeneous compartments with amounts of interchangeable material represented by non-negative variables [67].

In this chapter, we utilize such systems in order to describe the transport and accumulation of glucose, insulin and glucagon in the organism of a type 1 diabetic subject. In the section below, the mathematical model used in this thesis will be presented.

1.3 Mathematical Model

Several authors [61], [68], [69], [70], [71] believe a bihormonal closed-loop algorithm could provide a safe blood glucose regulation and reduce significantly the risk and time spent in hypoglycemic episodes [60] compared to usual insulin therapy.

The availability of a model that incorporates glucagon as a counter-regulatory hormone to insulin would allow more efficient design of bihormonal glucose controllers [61]. In this sense, an extended minimal model was proposed [66] to incorporate the glucagon effect.

For the sake of simplicity, we consider in the design of the controller only the reduced model [66]. Such assumption is reasonable since some dynamics among all presented in the extended model are, in general, faster than the dynamics of plasma glucose concentration, insulin action on glucose production and glucagon action on glucose production.

Therefore, the dynamics presented in [66] is now represented by:

$$\dot{x}_1(t) = -(S_G + x_2(t) - x_3(t))x_1(t) + S_G G_B + \frac{1}{t_{\text{maxG}} V} d(t)\,, \tag{16}$$

$$\dot{x}_2(t) = -p_2(t)x_2(t) + p_2(t)S_I(t)(u^+ - I_B)\,, \tag{17}$$

$$\dot{x}_3(t) = -p_3(t)x_3(t) + p_3(t)S_N(t)(u^- - N_B)\,, \tag{18}$$

$$y(t) = x_1(t)\,, \tag{19}$$

where $y(t)$ [mg/dL] is the output variable, $x_1(t)$ [mg/dL] is the plasma glucose concentration, $x_2(t)$ [min^{-1}] is the insulin action on glucose production, and $x_3(t)$ [min^{-1}] is the glucagon action on glucose production. $V = 1.7$ [dL/kg] is the glucose distribution volume. $u^+ \in \mathbb{R}^+$ [μU/dL] is the control action and represents the plasma insulin concentration, $u^- \in \mathbb{R}^+$ [pg/dL] is the control action and represents the plasma glucagon concentration, $d(t)$ [mg/kg] is the glucose concentration resulting from ingested meals and $S_G = 0.014$ [min^{-1}] is the glucose effectiveness per unit distribution volume. For sake of simplicity, the parameter $t_{maxG} = 69,6$ [min] was assumed constant, since its fluctuations are too slow, in general [66]. All other variables and parameters are described in Table 1, followed by its respective units and descriptions. Finally, we remark that if $u^+ \in \mathbb{R}^+$ and $u^- \in \mathbb{R}^+$, it means that the control signals are positive.

Table 1: Description of extended minimal model parameters.

Parameters	Description	Units
S_G	glucose effectiveness per unit distribution volume	[min^{-1}]
G_B	basal plasma glucose concentration	[mg/dL]
$t_{\text{max}\,G}(t)$	time-to-maximum glucose absorption	[min]
V	glucose distribution volume	[dL/kg]
$p_2(t)$	rate of disappearance of the interstitial insulin effect	[min^{-1}]
$S_I(t)$	insulin sensitivity	[min^{-1} per μ U/mL]
$I_B(t)$	basal plasma insulin concentration	[mU/dL]
$p_3(t)$	rate constant describing the dynamics of glucagon action	[min^{-1}]
$S_N(t)$	glucagon sensitivity	[min^{-1} per pg/mL]
$N_B(t)$	basal plasma glucagon concentration	[pg/mL]

The author of the extended model [66] identifies the model parameters for three detached periods of a same day in order to imitate the circadian rhythm of three real subjects.[5]. In this thesis, however, we have decided to work with a single virtual subject[6].

[5]The term "circadian rhythm" designates the period of approximately 24 hours in the course of which is based the biological cycle of almost all living beings [72].

[6]The subject $117 - 1$ presented in [66]. From this point on, the numerical values of all the model parameters will be refered to this subject. For detailed information about the model and its parameters, with the numerical values, we recommend the lecture of [66].

The mathematical description of the time-varying parameters is given bellow:

$$p_2(t) = 0,012\mathbb{1}(t) - 0,0081\mathbb{1}(t-300) + 0,0171\mathbb{1}(t-720) - 0,009\mathbb{1}(t-1080)\,, \tag{20}$$

$$p_3(t) = 0,017\mathbb{1}(t) - 0,001\mathbb{1}(t-300) + 0,123\mathbb{1}(t-720) - 0,122\mathbb{1}(t-1080)\,, \tag{21}$$

$$S_I(t) = [7,73\mathbb{1}(t) + 0,82\mathbb{1}(t-300) - 1,73\mathbb{1}(t-720) + 0,91\mathbb{1}(t-1080)] \times 10^{-4}\,, \tag{22}$$

$$S_N(t) = [1,38\mathbb{1}(t) + 0,58\mathbb{1}(t-300) - 1,15\mathbb{1}(t-720) + 0,57\mathbb{1}(t-1080)] \times 10^{-4}\,, \tag{23}$$

$$I_B(t) = 11,01\mathbb{1}(t) + 8,75\mathbb{1}(t-300) - 9,73\mathbb{1}(t-720) + 0,98\mathbb{1}(t-1080)\,, \tag{24}$$

$$N_B(t) = 46,30\mathbb{1}(t) + 1,83\mathbb{1}(t-300) + 11,10\mathbb{1}(t-720) - 12,93\mathbb{1}(t-1080)\,, \tag{25}$$

where $\mathbb{1}(t)$ is the unit step function. The time and the time delay in the unit step function are measured in minutes. Therefore, the functions $\mathbb{1}(t-300)$, $\mathbb{1}(t-720)$ and $\mathbb{1}(t-1080)$ denote changes in parameters (20)–(25) at 5:00, 12:00 and 18:00, respectively.

The minimum and maximum parameters values for (20)–(25) are respectively:

$$0,0039 \leq p_2(t) \leq 0,021\,, \tag{26}$$

$$0,016 \leq p_3(t) \leq 0,139\,, \tag{27}$$

$$6,82 \times 10^{-4} \leq S_I(t) \leq 8,55 \times 10^{-4}\,, \tag{28}$$

$$0,81 \times 10^{-4} \leq S_N(t) \leq 1,96 \times 10^{-4}\,, \tag{29}$$

$$10,03 \leq I_B(t) \leq 19,76\,, \tag{30}$$

$$46,30 \leq N_B(t) \leq 59,23\,. \tag{31}$$

During the development of the stability analysis, the system parameters will be considered uncertain in such a way that its bounds are known and described by

$$\underline{p}_2 < p_2(t) < \overline{p}_2\,, \quad \underline{p}_3 < p_3(t) < \overline{p}_3\,, \tag{32}$$

$$\underline{S}_I < S_I(t) < \overline{S}_I\,, \quad \underline{S}_N < S_N(t) < \overline{S}_N\,, \tag{33}$$

$$\underline{I}_B < I_B(t) < \overline{I}_B\,, \quad \underline{N}_B < N_B(t) < \overline{N}_B\,, \tag{34}$$

$$\underline{t}_{\text{maxG}} < t_{\text{maxG}}\,, \quad G_B < \overline{G}_B\,, \quad \underline{V} < V\,, \tag{35}$$

$$\underline{S_G} < S_G < \overline{S_G}\,. \tag{36}$$

Furthermore, we assume that

$$|d(t)| < \overline{d}\,, \quad |\dot{d}(t)| < \overline{\dot{d}}\,, \tag{37}$$

where $\overline{d}$ and $\overline{\dot{d}}$ are positive known constants for which (37) is satisfied, except for a zero measure set in the sense of Lebesgue.

At last, a couple of remarks concerning the hormones units are presented. Glucagon levels are reported as picogram per milliliter (pg/mL). Insulin is administrated in units, abbreviated U (international units). One unit of insulin is defined as the amount of insulin that will lower the blood glucose of a healthy 2 kg rabbit that has fasted for 24 hours to 45 mg/dL within 5 hours [73].

Proceeding forward, we present the control objective and the methodology utilized in order to reach it. The tools explored for this purpose will be duly discussed.

1.4 Methodology and Control Objectives

The goal of this project is to ensure the regulation of glycemia in a patient with T1DM. Mathematically, it can be represented through output error stabilization:

$$e(t) = G_B - x_1(t)\,, \tag{38}$$

where $G_B = 90$ mg/dL represents the desired setpoint. This value was chosen so that the glycemia of the patient with T1DM remained within the limits considered safe by the medical community: 80 and 100 mg/dL [38].

Among all the nonlinear control strategies available, we decided to work with Sliding Modes Controllers (SMC). The main advantage of a SMC relies on the fact that its design does not demand the precise knowledge of the model to be controlled. For controller design, it is sufficient that the upper and lower bounds of the plant parameters are known. The knowledge of upper bounds for disturbances is also required. In this sense, the proposed algorithm is said to be robust with respect to parametric uncertainties and exogenous disturbances. In this chapter, the food intake is considered an exogenous disturbance.

1.4.1 Glycemic Curve

An illustrative record of glycemia of a healthy subject in the course of 24 hours is depicted in Figure 2. It is about a glycemic curve of a healthy subject, whose organism is able to safely regulate the blood glucose, avoiding hypoglycemic and hyperglycemic cases [60].

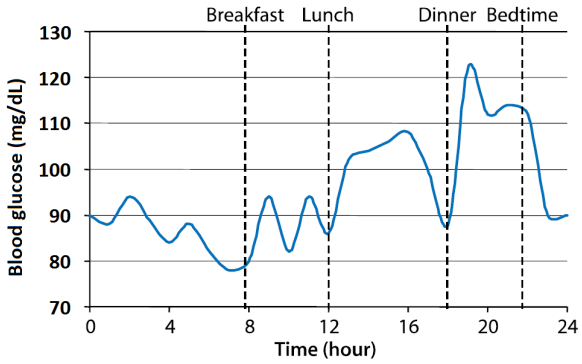

Figure 2: Glycemia of a health subject (figure adapted from [1])

Figure 3, in turn, illustrates the glycemic curve of a type 1 diabetic patient, who strives for regulate his blood glucose by regular practice of exercises, a balanced diet and multiple daily injections. This figure was obtained with the help a *FreeStyle Libre* sensor [74]. Through this graphic, we can remark that the standard open-loop insulin pump therapy is unable to maintain blood glucose regulated within safe limits during the 24 hours of the day.

The contrast between this type of therapy and closed-loop control strategy will become more evident in Section 1.10, when the simulation results of the control algorithms employed here will be presented. The comparison between Figure 2 and Figure 3 makes evident the undesirable effect that Diabetes Mellitus has on glycemic regulation.

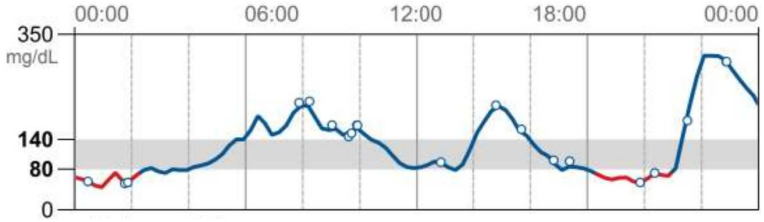

Figure 3: Blood glucose regulation of a DMT1 subject by means of a medical diet. The manufacturer of this sensor considers the safe blood glucose range to be between 80 and 140 [mg/dL], as indicated in the vertical axis.

1.5 Food Ingestion as Input Disturbances

In this research, it is desired that the patient's blood glucose be regulated over a period of 24 hours, which is equivalent to 1440 minutes. In this context, it is required for the patient to maintain a regular diet consisting of three meals a day, scheduled for the following times: 5:00, 12:00 and 18:00. The food intake modeling was proposed in [44] and [75] as:

$$d(t) = 80e^{-0,5(t-300)}\mathbb{1}(t-300) + 100e^{-0,5(t-720)}\mathbb{1}(t-720) + 70e^{-0,5(t-1080)}\mathbb{1}(t-1080)\,, \tag{39}$$

where $d(t)$ can be understood as an exogenous disturbance of the system. Therefore, it is assumed that each meal may represent a different rate of appearance of blood glucose. Figure 4 depicts the effect of meal intake over the patient glycemia.

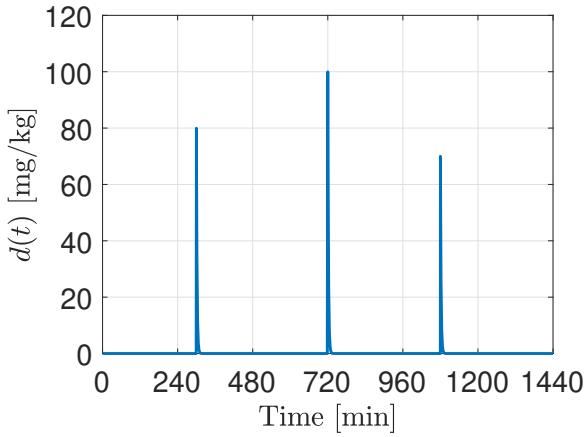

Figure 4: Glucose concentration resulting from ingested meals along the day.

Hereupon, observe the system (16)–(19). Note the disturbance appears in equation (16), whilst the positive and negative control actions, u^+ and u^-, respectively, appear in equations (17) and (18).

Thus, the disturbances are said to be *unmatched* because the control action does not appear in the same equation [34]. It generates an additional challenge in the controller design, since the control gain will have to upper bound the perturbation and its derivatives in amplitude.

1.6 Bihormonal Actuator

Sliding mode controllers have two control actions: a positive control action, u^+, and a negative control action, u^-. However, in this essay we are dealing with *strictly positive* systems, as discussed in Section 1.2. It means the so-called *positive* and *negative* must always assume positive values. Therefore, in this thesis, the positive control action is represented by the amount of insulin administered in the bloodstream, whilst the negative control action is represented by the amount of glucagon administered in the bloodstream. The algorithm decides which hormone should be injected into the patient at each moment, and this decision satisfies the following rule:

$$u^+ = \begin{cases} \varrho\,, & if \quad u > 0 \quad (\text{sgn}(\sigma) < 0) \\ 0\,, & \text{otherwise} \end{cases}, \tag{40}$$

$$u^- = \begin{cases} \varrho\,, & if \quad u < 0 \quad (\text{sgn}(\sigma) > 0) \\ 0\,, & \text{otherwise} \end{cases}, \tag{41}$$

where ϱ represents the controller modulation function, and σ represents the sliding variable. With rules (40)–(41) in mind, we can conclude that insulin and glucagon are never simultaneously administered.

1.7 First-Order Sliding Mode Control: Design and Stability Analysis

Sliding mode control is a well documented control technique, and its fundamentals can be found in [34] and [35].

In what follows, we present the local analysis of the first-order sliding mode controller, by means of the ideal sliding variable. Thus, it is assumed, initially, that the error derivatives are available.

Theorem 1. *Consider the system (16)–(19) with time varying parameters satisfying (20)–(25), with upper and lower bounds described by (32–(35), bounded disturbance given by (37) and error system (38) converging to zero. Thus, it is possible to find a sliding mode*

control law, u, given by:

$$u = -\varrho \mathrm{sgn}(\sigma(t))\,, \quad \varrho > 0\,, \tag{42}$$

$$\sigma(t) = \dot{e}(t) + l_0 e(t)\,, \quad l_0 > 0\,, \tag{43}$$

with a constant and sufficiently large modulation function, ϱ, and with such a sliding variable, $\sigma(t)$, that the ideal sliding mode, $\sigma(t) = 0$, occurs in finite time $t_s > 0$. Besides, under the sliding regime, the error convergence is exponential, i.e., $e(t) = e^{-l_0(t-t_s)}e(0)\,, \quad \forall t \geq t_s$.

Proof 1. *Consider the following Lyapunov function candidate*

$$V(t) = \sigma^2(t)\,, \tag{44}$$

where the time-derivative of V is given by $\dot{V}(t) = 2\sigma(t)\dot{\sigma}(t)$. Thus, with the aid of (43), one has:

$$\dot{V}(t) = 2\sigma(t)(\ddot{e}(t) + l_0\dot{e}(t))\,. \tag{45}$$

Differentiating the output error (38) with respect to time once and then twice yields:

$$\dot{e}(t) = -\dot{y}(t) = S_G x_1(t) + x_1(t)x_2(t) - x_1(t)x_3(t) - S_G G_B - \frac{1}{t_{\mathrm{maxG}} V} d(t)\,, \tag{46}$$

$$\begin{aligned}
\ddot{e}(t) =& \Big(- S_G^2 - p_2(t) S_I(t) I_B(t) + p_3(t) S_N(t) N_B(t) \Big) x_1(t) + S_G G_B x_2(t) \\
& - S_G G_B x_3(t) - \Big(2S_G + p_2(t) \Big) x_1(t) x_2(t) + \Big(2S_G + p_3(t) \Big) x_1(t) x_3(t) \\
& - x_1(t) x_2^2(t) - x_1(t) x_3^2(t) + 2 x_1(t) x_2(t) x_3(t) + \frac{1}{t_{\mathrm{maxG}} V} S_G d(t) \\
& + \frac{1}{t_{\mathrm{maxG}} V} x_2(t) d(t) - \frac{1}{t_{\mathrm{maxG}} V} x_3(t) d(t) - \frac{1}{t_{\mathrm{maxG}} V} \dot{d}(t) + S_G^2 G_B \\
& + p_2(t) S_I(t) x_1(t) u^+ - p_3(t) S_N(t) x_1(t) u^-\,.
\end{aligned} \tag{47}$$

The time-derivative of the sliding variable (43), after replacing (46)–(47), is given by:

$$\begin{aligned}
\dot{\sigma}(t) &= \ddot{e}(t) + l_0\dot{e}(t) \\
&= \Big(- S_G^2 - p_2(t)S_I(t)I_B(t) + p_3(t)S_N(t)N_B(t)\Big)x_1(t) + S_G G_B x_2(t) \\
&\quad - S_G G_B x_3(t) - \Big(2S_G + p_2(t)\Big)x_1(t)x_2(t) + \Big(2S_G + p_3(t)\Big)x_1(t)x_3(t) \\
&\quad - x_1(t)x_2^2(t) - x_1(t)x_3^2(t) + S_G^2 G_B + l_0 S_G x_1(t) + l_0 x_1(t)x_2(t) \\
&\quad - l_0 x_1(t)x_3(t) - l_0 S_G G_B + 2x_1(t)x_2(t)x_3(t) + \frac{1}{t_{\max\mathrm{G}}V} S_G d(t) \\
&\quad + \frac{1}{t_{\max\mathrm{G}}V} x_2(t)d(t) - \frac{1}{t_{\max\mathrm{G}}V} x_3(t)d(t) - \frac{1}{t_{\max\mathrm{G}}V}\dot{d}(t) - \frac{l_0}{t_{\max\mathrm{G}}V} d(t) \\
&\quad + p_2(t)S_I(t)x_1(t)u^+ - p_3(t)S_N(t)x_1(t)u^- \,, \qquad (48)
\end{aligned}$$

Therefore, the first derivative of the candidate Lyapunov function is given by:

$$\begin{aligned}
\dot{V}(t) =& 2\Big\{(-S_G^2 - p_2(t)S_I(t)I_B(t) + (p_3(t)S_N(t)N_B(t))x_1(t) + S_G G_B x_2(t))\sigma(t) \\
&- S_G G_B x_3(t)\sigma(t) - (2S_G + p_2(t))x_1(t)x_2(t)\sigma(t) + 2S_G x_1(t)x_3(t)\sigma(t) \\
&+ p_3(t)x_1(t)x_3(t)\sigma(t) + (2x_1(t)x_2(t)x_3(t) - x_1(t)x_2^2(t) + S_G^2 G_B)\sigma(t) \\
&- x_1(t)x_3^2(t)\sigma(t) + \frac{1}{t_{\max\mathrm{G}}V}([S_G + x_2(t) - x_3(t)]d(t) - \dot{d}(t))\sigma(t) \\
&+ l_0 S_G x_1(t)\sigma(t) + l_0 x_1(t)x_2(t)\sigma(t) - l_0 x_1(t)x_3(t)\sigma(t) - l_0 S_G G_B\sigma(t) \\
&- \frac{l_0}{t_{\max\mathrm{G}}V} d(t)\sigma(t) + p_2(t)S_I(t)x_1(t)u^+\sigma(t) - p_3(t)S_N(t)x_1(t)u^-\sigma(t)\Big\} \,. \qquad (49)
\end{aligned}$$

Note that (49) can be upper bounded by:

$$\begin{aligned}
\dot{V}(t) \leq 2\Big\{&(S_G^2 + p_2(t)S_I(t)I_B(t) + p_3(t)S_N(t)N_B(t))|x_1(t)||\sigma(t)| \\
&+ S_G G_B(|x_2(t)| + |x_3(t)|)|\sigma(t)| + (2S_G + p_2(t))|x_1(t)||x_2(t)||\sigma(t)| \\
&+ (2S_G + p_3(t))|x_1(t)||x_3(t)||\sigma(t)| + (2S_G + p_3(t))|x_1(t)||x_3(t)||\sigma(t)| \\
&+ |x_1(t)||x_2^2(t)||\sigma(t)| + |x_1(t)||x_3^2(t)||\sigma(t)| + 2|x_1(t)||x_2(t)||x_3(t)||\sigma(t)| \\
&+ \frac{1}{t_{\max\mathrm{G}}V}(S_G + |x_2(t)| + |x_3(t)|)|d(t)||\sigma(t)| + \frac{1}{t_{\max\mathrm{G}}V}|\dot{d}(t)||\sigma(t)| \\
&+ S_G^2 G_B|\sigma(t)| + l_0 S_G|x_1(t)||\sigma(t)| + l_0|x_1(t)||x_2(t)||\sigma(t)| \\
&+ l_0|x_1(t)||x_3(t)||\sigma(t)| + l_0 S_G G_B|\sigma(t)|\sigma(t) + \frac{l_0}{t_{\max\mathrm{G}}V}|d(t)||\sigma(t)| \\
&+ p_2(t)S_I(t)x_1(t)u^+\sigma(t) - p_3(t)S_N(t)x_1(t)u^-\Big\} \,. \qquad (50)
\end{aligned}$$

Since the system parameters are uncertain, by using the bounds (32)–(36), the inequality (50) can be upper bounded by:

$$\begin{aligned}\dot{V}(t) \leq & 2\Big\{\Big[(\bar{S}_G^2+\bar{p}_2\bar{S}_I\bar{I}_B+\bar{p}_3\bar{S}_N\bar{N}_B)|x_1(t)|+\bar{S}_G\bar{G}_B(|x_2(t)|+|x_3(t)|)\\ &+(2\bar{S}_G\bar{p}_2)|x_1(t)||x_2(t)|+(2\bar{S}_G+\bar{p}_3)|x_1(t)||x_3(t)|+|x_1(t)|x_2^2(t)\\ &+|x_1(t)|(x_3^2(t)+2|x_2(t)||x_3(t)|)+\frac{1}{\underline{t}_{\text{maxG}}\ \underline{V}}(\bar{S}_G+|x_2(t)|+|x_3(t)|)|d(t)|\\ &+\frac{1}{\underline{t}_{\text{maxG}}\ \underline{V}}|\dot{d}(t)|+\bar{S}_G^2\bar{G}_B+l_0\bar{S}_G|x_1(t)|\\ &+l_0|x_1(t)||x_2(t)|+l_0|x_1(t)||x_3(t)|+l_0\bar{S}_G\bar{G}_B+\frac{l_0}{\underline{t}_{\text{maxG}}\ \underline{V}}|d(t)|\Big]|\sigma(t)|\\ &+p_2(t)S_I(t)x_1(t)u^+\sigma(t)-p_3(t)S_N(t)x_1(t)u^-\sigma(t)\Big\}\,. \end{aligned}\tag{51}$$

The patient receives insulin ($u^+=\varrho$) if $u>0$. In this case, $\text{sgn}(\sigma)<0\rightarrow\sigma=-|\sigma|$ and $u^-=0$. So, the inequality (50) can be rewritten as:

$$\begin{aligned}\dot{V}(t) \leq & 2\Big\{(\bar{S}_G^2+\bar{p}_2\bar{S}_I\bar{I}_B+\bar{p}_3\bar{S}_N\bar{N}_B)|x_1(t)|+\bar{S}_G\bar{G}_B(|x_2(t)|+|x_3(t)|)\\ &+(2\bar{S}_G+\bar{p}_2)|x_1(t)||x_2(t)|+(2\bar{S}_G+\bar{p}_3)|x_1(t)||x_3(t)|+|x_1(t)|x_2^2(t)\\ &+|x_1(t)|x_3^2(t)+2|x_1(t)||x_2(t)||x_3(t)|+\frac{1}{\underline{t}_{\text{maxG}}\ \underline{V}}(|x_2(t)|+|x_3(t)|)|d(t)|\\ &+\frac{1}{\underline{t}_{\text{maxG}}\ \underline{V}}\bar{S}_G+\frac{1}{\underline{t}_{\text{maxG}}\ \underline{V}}|\dot{d}(t)|+\bar{S}_G^2\bar{G}_B+l_0\bar{S}_G|x_1(t)|+l_0|x_1(t)||x_2(t)|\\ &+l_0|x_1(t)||x_3(t)|+l_0\bar{S}_G\bar{G}_B+\frac{l_0}{\underline{t}_{\text{maxG}}\ \underline{V}}|d(t)|-p_2(t)S_I(t)x_1(t)\varrho\Big\}|\sigma(t)|\,. \end{aligned}\tag{52}$$

The patient receives glucagon ($u^-=\varrho$) if $u<0$. In this case, $\text{sgn}(\sigma)>0\rightarrow\sigma=|\sigma|$ and $u^+=0$. So, the inequality (50) can be rewritten as:

$$\begin{aligned}\dot{V}(t) \leq & 2\Big\{(\bar{S}_G^2+\bar{p}_2\bar{S}_I\bar{I}_B+\bar{p}_3\bar{S}_N\bar{N}_B)|x_1(t)|+\bar{S}_G\bar{G}_B(|x_2(t)|+|x_3(t)|)\\ &+(2\bar{S}_G+\bar{p}_2)|x_1(t)||x_2(t)|+(2\bar{S}_G+\bar{p}_3)|x_1(t)||x_3(t)|+|x_1(t)|x_2^2(t)\\ &+|x_1(t)|x_3^2(t)+2|x_1(t)||x_2(t)||x_3(t)|+\frac{1}{\underline{t}_{\text{maxG}}\ \underline{V}}(|x_2(t)|+|x_3(t)|)|d(t)|\\ &+\frac{1}{\underline{t}_{\text{maxG}}\ \underline{V}}\bar{S}_G+\frac{1}{\underline{t}_{\text{maxG}}\ \underline{V}}|\dot{d}(t)|+\bar{S}_G^2\bar{G}_B+l_0\bar{S}_G|x_1(t)|+l_0|x_1(t)||x_2(t)|\\ &+l_0|x_1(t)||x_3(t)|+l_0\bar{S}_G\bar{G}_B+\frac{l_0}{\underline{t}_{\text{maxG}}\ \underline{V}}|d(t)|-p_3(t)S_N(t)x_1(t)\varrho\Big\}|\sigma(t)|\,. \end{aligned}\tag{53}$$

Since x_1 stands for glucose, it is straightforward to conclude that at least $x_1>1\,,\forall t$.

Therefore, the inequalities (52) and (53) can be upper bounded by

$$\begin{aligned}\dot{V}(t) \leq 2\Big\{&(\bar{S}_G^2+\bar{p}_2\bar{S}_I\bar{I}_B+\bar{p}_3\bar{S}_N\bar{N}_B)|x_1(t)|+\bar{S}_G\bar{G}_B(|x_2(t)|+|x_3(t)|+l_0)\\&+(2\bar{S}_G+\bar{p}_2)|x_1(t)||x_2(t)|+(2\bar{S}_G+\bar{p}_3)|x_1(t)||x_3(t)|+|x_1(t)|x_2^2(t)\\&+|x_1(t)|x_3^2(t)+2|x_1(t)||x_2(t)||x_3(t)|+\frac{1}{\underline{t}_{\text{maxG}}\ \underline{V}}(|x_2(t)|+|x_3(t)|)|d(t)|\\&+\frac{1}{\underline{t}_{\text{maxG}}\ \underline{V}}\bar{S}_G+\frac{1}{\underline{t}_{\text{maxG}}\ \underline{V}}|\dot{d}(t)|+\bar{S}_G^2\bar{G}_B+l_0\bar{S}_G|x_1(t)|+l_0|x_1(t)||x_2(t)|\\&+l_0|x_1(t)||x_3(t)|+\frac{l_0}{\underline{t}_{\text{maxG}}\ \underline{V}}|d(t)|-\min\{\underline{p}_2,\underline{p}_3\}\min\{\underline{S}_I,\underline{S}_N\}\varrho\Big\}|\sigma(t)|\,.\end{aligned}\tag{54}$$

From (54), an upper bound to the time-derivative of the Lyapunov function can be described by:

$$\begin{aligned}\dot{V}(t) \leq 2\Bigg\{&\left(\bar{S}_G^2+\bar{p}_2\bar{S}_I\bar{I}_B+\bar{p}_3\bar{S}_N\bar{N}_B+2\bar{S}_G\bar{G}_B+l_0\bar{S}_G+\frac{2}{\underline{t}_{\text{maxG}}\ \underline{V}}|d(t)|\right)|x(t)|\\&+(4\bar{S}_G+\bar{p}_2+\bar{p}_3+2l_0)|x(t)|^2+4|x(t)|^3+\frac{\bar{S}_G+l_0}{\underline{t}_{\text{maxG}}\ \underline{V}}|d(t)|+\frac{1}{\underline{t}_{\text{maxG}}\ \underline{V}}|\dot{d}(t)|\\&+\bar{S}_G^2\bar{G}_B+l_0\bar{S}_G\bar{G}_B-\min\{\underline{p}_2,\underline{p}_3\}\min\{\underline{S}_I,\underline{S}_N\}\varrho\Bigg\}|\sigma(t)|\,.\end{aligned}\tag{55}$$

The meal disturbance, $d(t)$, and its first time-derivative, $\dot{d}(t)$, are bounded by some real positive number described in (37), such that,

$$\begin{aligned}\dot{V}(t) \leq 2\Bigg\{&\left(\bar{S}_G^2+\bar{p}_2\bar{S}_I\bar{I}_B+\bar{p}_3\bar{S}_N\bar{N}_B+2\bar{S}_G\bar{G}_B+l_0\bar{S}_G+\frac{2}{\underline{t}_{\text{maxG}}\ \underline{V}}\bar{d}\right)|x(t)|\\&+(4\bar{S}_G+\bar{p}_2+\bar{p}_3+2l_0)|x(t)|^2+4|x(t)|^3+\frac{\bar{S}_G+l_0}{\underline{t}_{\text{maxG}}\ \underline{V}}\bar{d}+\frac{1}{\underline{t}_{\text{maxG}}\ \underline{V}}\bar{\dot{d}}\\&+\bar{S}_G^2\bar{G}_B+l_0\bar{S}_G\bar{G}_B-\min\{\underline{p}_2,\underline{p}_3\}\min\{\underline{S}_I,\underline{S}_N\}\varrho\Bigg\}|\sigma(t)|\,.\end{aligned}\tag{56}$$

Let us define $k_1=\bar{S}_G^2+\bar{p}_2\bar{S}_I\bar{I}_B+\bar{p}_3\bar{S}_N\bar{N}_B+2\bar{S}_G\bar{G}_B+l_0\bar{S}_G+\frac{2}{\underline{t}_{\text{maxG}}\ \underline{V}}\bar{d}$, $k_2=4\bar{S}_G+\bar{p}_2+\bar{p}_3+2l_0$, $k_3=4$ and $k_4=\frac{\bar{S}_G+l_0}{\underline{t}_{\text{maxG}}\ \underline{V}}\bar{d}+\frac{1}{\underline{t}_{\text{maxG}}\ \underline{V}}\bar{\dot{d}}+\bar{S}_G^2\bar{G}_B+l_0\bar{S}_G\bar{G}_B$. Thus, equation (56) becomes:

$$\begin{aligned}\dot{V}(t) \leq 2\Big\{&k_1|x(t)|+k_2|x(t)|^2+k_3|x(t)|^3+k_4\\&-\min\{\underline{p}_2,\underline{p}_3\}\min\{\underline{S}_I,\underline{S}_N\}\varrho\Big\}|\sigma(t)|\,.\end{aligned}\tag{57}$$

It is worth mentioning that the state is bounded, since we are dealing with a biological

system. Thus, we suppose there exists a known upper bound such that the inequality $|x(t)| < \chi$ *is satisfied. Therefore, equation (57) can be rewritten as*

$$\dot{V}(t) \leq 2\left\{k_1\chi + k_2\chi^2 + k_3\chi^3 + k_4 - \min\{\underline{p}_2, \underline{p}_3\}\min\{\underline{S}_I, \underline{S}_N\}\varrho\right\}|\sigma(t)|\,. \tag{58}$$

The modulation function is defined as

$$\varrho = \frac{k_1\chi + k_2\chi^2 + k_3\chi^3 + k_4 + \delta}{\min\{\underline{p}_2, \underline{p}_3\}\min\{\underline{S}_I, \underline{S}_N\}}\,, \quad \delta > 0\,. \tag{59}$$

If (59) is replaced into (58), then we can readily obtain

$$\dot{V}(t) \leq -2\delta|\sigma(t)|\,, \quad t \geq 0\,. \tag{60}$$

Let $\tilde{\sigma}(t) := |\sigma(t)| = \sqrt{V(t)}$ *be the auxiliary variable. Thus, we have* $\dot{\tilde{\sigma}}(t) = \frac{\dot{V}(t)}{2\sqrt{V(t)}}$. *Proceeding forward, we divide both sides of (60) by* $2\sqrt{V(t)}$, *which implies that*

$$\frac{\dot{V}(t)}{2\sqrt{V(t)}} \leq -2\delta\frac{|\sigma(t)|}{2\sqrt{V(t)}}\,, \tag{61}$$

which is identical to

$$\dot{\tilde{\sigma}}(t) \leq -\delta\,, \quad t \geq 0\,. \tag{62}$$

By using the Comparison Lemma, [76], pp.84-87, there exists an upper bound $\bar{\sigma}(t)$ *of* $\tilde{\sigma}(t)$ *that satisfies the differential equation*

$$\dot{\bar{\sigma}}(t) = -\delta\,, \quad \bar{\sigma}(0) = \tilde{\sigma}(0) \geq 0\,, \quad t \geq 0\,. \tag{63}$$

Integrating both sides of equation (63) yields

$$\bar{\sigma}(t) - \bar{\sigma}(0) = -\delta t\,, \quad t \geq 0\,. \tag{64}$$

Therefore, the following inequality holds:

$$\bar{\sigma}(t) = -\delta t + \bar{\sigma}(0)\,, \quad t \geq 0\,. \tag{65}$$

Since $\bar{\sigma} \geq 0$ is continuous, $\sigma(t)$ becomes identically null $\forall t \geq t_1 = \delta^{-1}\bar{\sigma}(0)$. Proceeding forward, we conclude that there exists a finite time $0 < t_s \leq t_1$, where the sliding mode starts such that $\sigma(t) = 0$, $\forall t \geq t_s$. From (43), we can conclude that $\dot{e} = -l_0 e$ and then the output error $e(t)$ converges exponentially to zero. □

1.7.1 Boundary Layer for Chattering Alleviation

There are some problems that are intrinsic to the traditional sliding mode controller, such as: discontinuous control action and the so-called *chattering* effect. In order to mitigate these effects, we utilize the boundary layer technique [77].

The boundary layer implementation occurs through the control law design. In this sense, instead of using the relay, we use a control action given by the following law:

$$u = -\varrho \frac{\hat{\sigma}}{|\hat{\sigma}| + \delta}\,, \tag{66}$$

where $0 < \delta < 1$. Let us call $f(\hat{\sigma}) = \frac{\hat{\sigma}}{|\hat{\sigma}|+\delta}$. Thus, $u = -\varrho f(\hat{\sigma})$. Observe that if $\delta = 0$, $f(\hat{\sigma}) = \text{sgn}(\hat{\sigma})$, and then both function $f(\hat{\sigma})$ and control action u are discontinuous. By the other hand, according to Figure 5, when $\delta \neq 0$, the function $f(\hat{\sigma})$ is continuous and so it is the control action u.

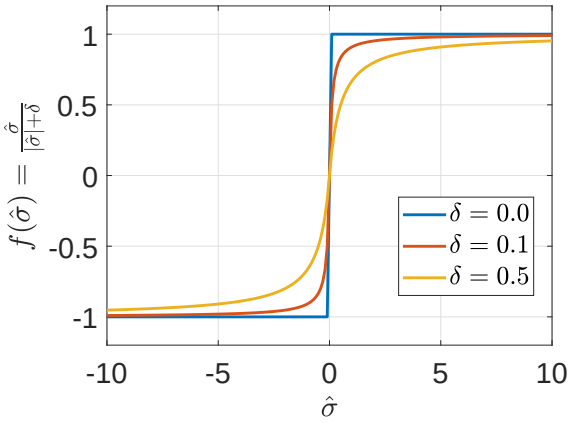

Figure 5: Graphic of function $f(\hat{\sigma})$ for different values of δ, according to (66).

Proceeding this way, attenuation of chattering effect is expected to be achieved.

1.8 Terminal Sliding Mode Control: Design and Stability Analysis

The Non-Singular Terminal SMC differs from the First-Order SMC primarily for two reasons. First, its sliding surface is a non-linear function of the error state variables. Second, while exponential convergence is guaranteed for the first order SMC when the closed-loop system remains on the sliding surface, the non-singular terminal algorithm is able to bring the state to the origin in finite-time ($e \equiv \dot{e} \equiv 0$) [78].

Theorem 2. *Consider the system (16)–(19) with time varying parameters satisfying (20)–(25), with upper and lower bounds described by (32–(35), bounded disturbance given by (37) and error system (38) converging to zero. Thus, it is possible to find a sliding mode control law, u, given by:*

$$u = -\varrho \text{sgn}\left(\sigma\right) , \quad \varrho > 0 , \tag{67}$$

$$\sigma(t) = e(t) + \frac{1}{\beta}\dot{e}^{p/q}(t) , \tag{68}$$

where $\beta = 2$, $p = 5$ and $q = 3$, such that the ideal sliding mode in $\sigma(t) = 0$ occurs in finite time. Besides, under the sliding regime, the error convergence occurs in finite time.

Proof 2. *Consider the following Lyapunov function candidate*

$$V(t) = \sigma^2(t) , \tag{69}$$

with $\sigma(t)$ given in (68). The time-derivative of (69) is

$$\begin{aligned}
\dot{V}(t) = 2 \Bigg\{ \Bigg[& S_G x_1(t) + x_1(t)x_2(t) - x_1(t)x_3(t) - S_G G_B - \frac{1}{t_{\text{maxG}} V} d(t) \\
& + \frac{1}{\beta}\frac{p}{q}\left(S_G x_1(t) + x_1(t)x_2(t) - x_1(t)x_3(t) - S_G G_B - \frac{1}{t_{\text{maxG}} V} d(t) \right)^{\frac{p-q}{q}} \times \\
& \times \left[(-S_G^2 - p_2 S_I I_B + p_3 S_N N_B) x_1(t) + S_G G_B (x_2(t) - x_3(t)) - x_1(t) x_3^2(t) \right. \\
& \left. - (2S_G + p_2) x_1(t) x_2(t) + (2S_G + p_3) x_1(t) x_3(t) - x_1(t) x_2^2(t) - x_3(t) \right] d(t) \\
& + 2 x_1(t) x_2(t) x_3(t) + \frac{1}{t_{\text{maxG}} V} \left(S_G + x_2(t) - \frac{1}{t_{\text{maxG}} V} \dot{d}(t) \right) \Bigg] \sigma(t) + \\
& \frac{1}{\beta}\frac{p}{q} \left(S_G x_1(t) + x_1(t)x_2(t) - x_1(t)x_3(t) - S_G G_B - \frac{1}{t_{\text{maxG}} V} d(t) \right)^{\frac{p-q}{q}} \times \\
& \times \left(p_2 S_I x_1(t) u^+ - p_3 S_N x_1(t) u^- \right) \sigma(t) \Bigg\} .
\end{aligned} \tag{70}$$

Insulin will be delivered to the patient ($u^+ = \varrho$) if $u > 0$. In this case, $\mathrm{sgn}(\sigma) < 0 \rightarrow \sigma = -|\sigma|$ *and* $u^- = 0$. *Glucagon will be delivered to the patient ($u^- = \varrho$) if $u < 0$. In this case,* $\mathrm{sgn}(\sigma) > 0 \rightarrow \sigma = |\sigma|$ *and* $u^+ = 0$. *Hence, for the sake of simplicity, we assume that: (i) $x_1(t) > 1$; (ii) it is always possible to find k_G sufficiently small; and (iii)* $\left(S_G x_1(t) + x_1(t)x_2(t) - x_1(t)x_3(t) - S_G G_B - \frac{1}{t_{\mathrm{maxG}} V} d(t)\right)^{\frac{p-q}{q}} \geq k_G \left(S_G G_B\right)^{\frac{p-q}{q}}$, *the equality (70) can be upper bounded by:*

$$
\begin{aligned}
\dot{V}(t) \leq & 2\Bigg\{\Bigg[S_G|x_1(t)| + |x_1(t)||x_2(t)| + |x_1(t)||x_3(t)| + S_G G_B \\
& + \frac{1}{t_{\mathrm{maxG}} V}|d(t)| + \frac{1}{\beta}\frac{p}{q}\Bigg(S_G|x_1(t)| + |x_1(t)||x_2(t)| + |x_1(t)||x_3(t)| \\
& + S_G G_B + \frac{1}{t_{\mathrm{maxG}} V}|d(t)|\Bigg)^{\frac{p-q}{q}}\Bigg((S_G^2 + p_2 S_I I_B + p_3 S_N N_B)|x_1(t)| \\
& + S_G G_B(|x_2(t)| + |x_3(t)|) + (2S_G + p_2)|x_1(t)||x_2(t)| \\
& + (2S_G + p_3)|x_1(t)||x_3(t)| + |x_1(t)|(|x_2(t)|^2 + |x_3(t)|^2) \\
& + 2|x_1(t)||x_2(t)||x_3(t)| + \frac{1}{t_{\mathrm{maxG}} V}(S_G + |x_2(t)| + |x_3(t)|)|d(t)| \\
& + \frac{1}{t_{\mathrm{maxG}} V}|\dot{d}(t)|\Bigg) - \frac{1}{\beta}\frac{p}{q}\left(S_G G_B\right)^{\frac{p-q}{q}} \min\{\underline{p}_2, \underline{p}_3\} \min\{\underline{S}_I, \underline{S}_N\}\varrho\Bigg]\Bigg\}. \qquad (71)
\end{aligned}
$$

By using the bounds (32)–(35), $|x(t)| < \chi$, $|d(t)| < \bar{d}$ *and* $|\dot{d}(t)| < \bar{\dot{d}}$ *in (71), it is possible to find*

$$
\begin{aligned}
\dot{V}(t) \leq & 2\Bigg\{\Bigg[\bar{S}_G\chi + 2\chi^2 + \bar{S}_G\bar{G}_B + \frac{1}{\underline{t_{\mathrm{maxG}}}\ \underline{V}}\bar{d} \\
& + \frac{1}{\beta}\frac{p}{q}\left(\bar{S}_G\chi + 2\chi^2 + \bar{S}_G\bar{G}_B + \frac{1}{\underline{t_{\mathrm{maxG}}}\ \underline{V}}\bar{d}\right)^{\frac{p-q}{q}} \times \\
& \left(\left(\bar{S}_G^2 + 2\bar{p}_2\bar{S}_I\bar{I}_B + \bar{p}_3\bar{S}_N\bar{N}_B + 2\bar{S}_G\bar{G}_B + \frac{1}{\underline{t_{\mathrm{maxG}}}\ \underline{V}}\right)\chi\right. \\
& \left. + (4\bar{S}_G + \bar{p}_2 + \bar{p}_3)\chi^2 + 4\chi^3 + \frac{\bar{S}_G\bar{d} + \bar{\dot{d}}}{\underline{t_{\mathrm{maxG}}}\ \underline{V}}\right) \\
& - \frac{k_G}{\beta}\frac{p}{q}\left(\underline{S}_G\underline{G}_B\right)^{\frac{p-q}{q}} \min\{\underline{p}_2, \underline{p}_3\} \min\{\underline{S}_I, \underline{S}_N\}\varrho\Bigg]\Bigg\}. \qquad (72)
\end{aligned}
$$

Defining $\bar{\chi}$ *as*

$$\begin{aligned}\bar{\chi} &= \bar{S}_G\chi + 2\chi^2 + \bar{S}_G\bar{G}_B + \frac{1}{\underline{t_{\text{maxG}}}\ \underline{V}}\bar{d} \\ &+ \frac{1}{\beta}\frac{p}{q}\left(\bar{S}_G\chi + 2\chi^2 + \bar{S}_G\bar{G}_B + \frac{1}{\underline{t_{\text{maxG}}}\ \underline{V}}\bar{d}\right)^{\frac{p-q}{q}} \times \\ &\times \left(\left(\bar{S}_G^2 + 2\bar{p}_2\bar{S}_I\bar{I}_B + \bar{p}_3\bar{S}_N\bar{N}_B + 2\bar{S}_G\bar{G}_B + \frac{1}{\underline{t_{\text{maxG}}}\ \underline{V}}\right)\chi\right. \\ &\left.+(4\bar{S}_G + \bar{p}_2 + \bar{p}_3)\chi^2 + 4\chi^3 + \frac{\bar{S}_G\bar{d} + \dot{\bar{d}}}{\underline{t_{\text{maxG}}}\ \underline{V}}\right), \end{aligned} \tag{73}$$

yields

$$\dot{V}(t) \leq 2\left\{\left[\bar{\chi} - \frac{k_G}{\beta}\frac{p}{q}\left(\underline{S}_G\underline{G}_B\right)^{\frac{p-q}{q}}\min\{\underline{p}_2, \underline{p}_3\}\min\{\underline{S}_I, \underline{S}_N\}\varrho\right]\right\}. \tag{74}$$

Then, defining the modulation function ϱ *conveniently as*

$$\varrho = \frac{\bar{\chi} + \delta}{\frac{k_G}{\beta}\frac{p}{q}\left(\underline{S}_G\underline{G}_B\right)^{\frac{p-q}{q}}\min\{\underline{p}_2, \underline{p}_3\}\min\{\underline{S}_I, \underline{S}_N\}}, \quad \delta > 0, \tag{75}$$

we can guarantee that the derivative of (69) satisfies inequality

$$\dot{V}(t) \leq -2\delta|\sigma(t)|. \tag{76}$$

Defining the auxiliary variable $\tilde{\sigma}(t) := |\sigma(t)| = \sqrt{V(t)}$*, we can readily obtain* $\dot{\tilde{\sigma}}(t) = \frac{\dot{V}(t)}{2\sqrt{V(t)}}$*. Next, dividing both sides of (76) by* $2\sqrt{V}(t)$*, yields*

$$\frac{\dot{V}(t)}{2\sqrt{V(t)}} \leq -2\delta\frac{|\sigma(t)|}{2\sqrt{V(t)}}, \tag{77}$$

that is identically equal to

$$\dot{\tilde{\sigma}}(t) \leq -\delta, \quad t \geq 0. \tag{78}$$

Using the comparison theorem, there is an upper bound $\bar{\sigma}(t)$ *of* $\tilde{\sigma}(t)$ *satisfying the*

differential equation

$$\dot{\bar{\sigma}}(t) = -\delta\,, \quad \bar{\sigma}(0) = \tilde{\sigma}(0) \geq 0\,, \quad t \geq 0\,. \tag{79}$$

Integrating both sides of equation (79) yields

$$\bar{\sigma}(t) - \bar{\sigma}(0) = -\delta t\,, \quad t \geq 0\,. \tag{80}$$

Thus, the following equality holds:

$$\bar{\sigma}(t) = -\delta t + \bar{\sigma}(0)\,, \quad t \geq 0\,. \tag{81}$$

Since $\bar{\sigma} \geq 0$ is a continuous signal, the variable $\sigma(t)$ becomes identically null $\forall t \geq t_1 = \delta^{-1}\bar{\sigma}(0)$. Thereby, one can conclude that there exists a finite time $0 < t_s \leq t_1$, where the sliding mode starts, such that $\sigma(t) = 0$ and $\dot{\sigma}(t) = 0$, $\forall t \geq t_s$. From (68), one can conclude that

$$|e(t)| = \frac{1}{\beta}\sqrt[p-q]{\left[\sqrt[p]{(\beta|e_0|)^{(p-q)}} - \beta\frac{(p-q)}{p}(t-t_0)\right]^p}\,, \quad \forall t \geq t_f\,, \tag{82}$$

where $t_f = t_s + \frac{p\sqrt[p]{(\beta|e_0|)^{(p-q)}}}{\beta(p-q)}$ and then the error $e(t)$ converges to zero in finite time, since the sliding variable σ becomes identically zero. □

1.8.1 Continuous Non-singular Terminal Sliding Mode Control for Chattering Alleviation

The extension of the output feedback to the Continuous Non-Singular Terminal Sliding Mode Algorithm (CNTSMA) can be obtained by following the steps introduced by [79]. It can be understood as a combination of a super-twisting algorithm [80] with a non-singular terminal SMC and written as:

$$\begin{aligned} u = &- k_1 \left|\zeta_1 + k_2|e|^{2/3}\mathrm{sgn}(e)\right|^{1/2} \mathrm{sgn}\left(\zeta_1 + k_2|e|^{2/3}\mathrm{sgn}(e)\right) \\ &- k_3 \int_0^t \mathrm{sgn}\left(\zeta_1 + k_2|e|^{2/3}\mathrm{sgn}(e)\right) d\tau\,, \end{aligned} \tag{83}$$

where $k_1 > 0$, $k_2 > 0$ and $k_3 > 0$ are appropriate constants.

1.9 HOSM Exact Differentiators for Output Feedback

In this chapter, it was chosen to work with two different control strategies called First-Order Sliding Mode Control and Non-Singular Terminal Sliding Modes Control. An issue that arises in this context is the necessity of error derivative signal in Theorems 1 and 2. In other words, the authors is assuming the state x_1 (the plasma glucose concentration) is available, but the states x_2 (the insulin action on glucose production) and x_3 (the glucagon action on glucose production) are not measurable. Nevertheless, this signal is not available directly. In this section, an exact differentiator based on High-Order Sliding Modes (HOSM) is applied to overcome this drawback. Besides its capability to provide the exact derivative of the output error $e \in \mathbb{R}$, it ensures the attenuation of small high frequency noises [81]. Its structure is given by:

$$\begin{aligned}
\dot{\zeta}_0 &= v_0 = -\lambda_0 C^{\frac{1}{p+1}} |\zeta_0 - e(t)|^{\frac{p}{p+1}} \operatorname{sgn}(\zeta_0 - e(t)) + \zeta_1, \\
&\vdots \\
\dot{\zeta}_i &= v_i = -\lambda_i C^{\frac{1}{p-i+1}} |\zeta_i - v_{i-1}|^{\frac{p-i}{p-i+1}} \operatorname{sgn}(\zeta_i - v_{i-1}) + \zeta_{i+1}, \\
&\vdots \\
\dot{\zeta}_p &= -\lambda_p C \operatorname{sgn}(\zeta_p - v_{p-1}) \,,
\end{aligned} \tag{84}$$

where λ_i are appropriate constants, chosen recursively; C is an appropriate constant, such that $C \geq |e^{(\rho)}(t)|$; the state is described by $\zeta = [\zeta_0,\ \ldots,\ \zeta_{\rho-1}]^T$; and $p = \rho - 1$ represents the order of the differentiator. Therefore, the following equalities

$$\zeta_0 = e(t) \,, \quad \zeta_i = e^{(i)}(t) \,, \quad i = 1 \,, \ldots \,, p \,, \tag{85}$$

are established in finite time [81], provided that the signal, $e^{(\rho)}(t)$, be uniformly bounded, as assumed in the HOSM differentiator.

As $\rho = 2$, knowing that the plant has dynamics given by (16)–(19), from the

regulation error (38), it is possible to show that the following inequality is satisfied:

$$\begin{aligned}
|\ddot{e}(t)| &= |(-S_G^2 - p_2 S_I I_B + p_3 S_N N_B) x_1(t) \\
&\quad + S_G G_B (x_2(t) - x_3(t)) - (2S_G + p_2) x_1(t) x_2(t) \\
&\quad + (2S_G + p_3) x_1(t) x_3(t) - x_1(t) x_2^2(t) - x_1(t) x_3^2(t) \\
&\quad + 2x_1(t) x_2(t) x_3(t) + \frac{d(t)}{t_{\mathrm{maxG}} V} (S_G + x_2(t) - x_3(t)) \\
&\quad - \frac{\dot{d}(t)}{t_{\mathrm{maxG}} V} + S_G^2 G_B + p_2 S_I x_1(t) u^+ - p_3 S_N x_1(t) u^- | \\
&\leq \big(\bar{S}_G^2 + \bar{p}_2 \bar{S}_I \bar{I}_B + \bar{p}_3 \bar{S}_N \bar{N}_B + 2\bar{S}_G \bar{G}_B + \frac{2\bar{d}}{\underline{t}_{\mathrm{maxG}}\, \underline{\mathrm{V}}} \\
&\quad + \max\{\bar{p}_2, \bar{p}_3\} + \max\{\bar{S}_I, \bar{S}_N\} \varrho \big) \chi \\
&\quad + (4\bar{S}_G + \bar{p}_2 + \bar{p}_3) \chi^2 + 4\chi^3 + \frac{\bar{S}_G \bar{d} + \bar{\dot{d}}}{\underline{t}_{\mathrm{maxG}}\, \underline{\mathrm{V}}} + \bar{S}_G^2 \bar{G}_B \,, \qquad (86)
\end{aligned}$$

where the parameters are upper bounded by (32)–(36), the disturbance, $d(t)$, and its derivative, $\dot{e}(t)$, satisfy (37) and the state norm is upper bounded at least locally, by $|x(t)| < \chi$. Assuming that these upper bounds are constant, and are available for designing the controller, an upper bound for the absolute value of the second time-derivative of $e(t)$ can be obtained through

$$\begin{aligned}
C &= \bigg(\bar{S}_G^2 + \bar{p}_2 \bar{S}_I \bar{I}_B + \bar{p}_3 \bar{S}_N \bar{N}_B + 2\bar{S}_G \bar{G}_B + \frac{2\bar{d}}{\underline{t}_{\mathrm{maxG}}\, \underline{\mathrm{V}}} \\
&\quad + \max\{\bar{p}_2, \bar{p}_3\} \max\{\bar{S}_I, \bar{S}_N\} \varrho \bigg) \chi + (4\bar{S}_G + \bar{p}_2 + \bar{p}_3) \chi^2 \\
&\quad + 4\chi^3 + \frac{\bar{S}_G \bar{d} + \bar{\dot{d}}}{\underline{t}_{\mathrm{maxG}}\, \underline{\mathrm{V}}} + \bar{S}_G^2 \bar{G}_B \,. \qquad (87)
\end{aligned}$$

Throughout this chapter, the following exact differentiator will be used:

$$\dot{\zeta}_0 = v_0 = -\lambda_0 C^{\frac{1}{2}} |\zeta_0 - e(t)|^{\frac{1}{2}} \mathrm{sgn}(\zeta_0 - e(t)) + \zeta_1, \qquad (88)$$

$$\dot{\zeta}_1 = -\lambda_1 C \mathrm{sgn}(\zeta_1 - v_0) \,, \qquad (89)$$

with $\lambda_0 = 5$ and $\lambda_1 = 3$ and gain C given in (87).

The values that have been used in implementing the control system and its parameters are given by: $\underline{\mathrm{p}}_2 = 0.003$ [min^{-1}], $\bar{p}_2 = 0.03$ [min^{-1}]; $\underline{\mathrm{p}}_3 = 0.01$ [min^{-1}]; $\bar{p}_3 = 0.14$ [min^{-1}]; $\underline{\mathrm{S}}_N = 0.8 \times 10^{-4}$ [min^{-1} per pg/mL]; $\bar{S}_N = 2 \times 10^{-4}$ [min^{-1} per

pg/mL]; $\underline{S}_I = 6.8 \times 10^{-4}$ [min^{-1} per μ U/mL]; $\bar{S}_I = 8.6 \times 10^{-4}$ [min^{-1} per μ U/mL]; $\bar{S}_G = 0.015$ [min^{-1}]; $\bar{N}_B = 60$ [pg/mL]; $\bar{I}_B = 20$ [mU/dL]; $\underline{V} = 1.5$ [dL/kg]; $\underline{t}_{\text{maxG}} = 65$ [min]; $\bar{d} = 110$ [mg/kg]; $\bar{\dot{d}} = 60$ [mg/kg per min] and $\varrho = 100$. These values were chosen from the numeric values of the parameters (20)–(25) which, in turn, can be consulted in [66].

1.10 Numerical Examples

In this section, the four strategies presented so far have their performances evaluated by simulation results: the traditional sliding mode controller (42)-(43) and the non-singular terminal sliding modes control (67)-(68), which have a discontinuous control action; the sliding mode controller with *boundary layer* (66) and the continuous non-singular terminal sliding modes control (83) whose control action are smooth.

Concerning the plant, the parameters values were chosen according to [66] and are described as follows: $S_G = 0.014$ [min^{-1}], $t_{maxG} = 69.6$ [min], $V = 1.7$ [dL/kg], $p_2 = 0.012$ [min^{-1}]; $p_3 = 0.017$ [min^{-1}]; $S_I = 7.73 \times 10^{-4}$ [min^{-1} per μ U/mL]; $S_N = 1.38 \times 10^{-4}$ [min^{-1} per pg/mL]; $I_B = 11.01$ [mU/dL] and $N_B = 46.30$ [pg/mL]. The desired setpoint was defined as $G_B = 90$ [mg/dL], as discussed in Section 1.3, and the initial condition of the glycaemia was arbitrarily chosen as $G_0 = 120$ [mg/dL]. The major concern was to define an initial condition that were different from the setpoint so as to attest the controllers performance. The initial condition of variables $x_2(t)$ [min^{-1}] and $x_3(t)$ [min^{-1}] were set as $x_2(0) = x_3(0) = 0$, as recommended in [66].

In what concerns the exact differentiator, the gain was defined as $C = 100$; the parameters as $\lambda_0 = 5$, $\lambda_1 = 3$; and the initial conditions as $\zeta_0(0) = 0$ and $\zeta_1(0) = 0$. The simulation time was set as $1,440$, since one desires to safely regulate the patient's blood glucose over a period of 24 hours, which is equivalent to $1,440$ minutes. At last, the sampling step was made equal to 10^{-3} s.

1.10.1 Discontinuous FOSMC with Estimate of Sliding Variable Using Exact Differentiator

Although Theorem 1 shows that it is possible to find a constant ϱ that locally guarantees the sliding mode, the control law (42)–(43) cannot be implemented, since

signal $\dot{e}$ is not available. Thus, recalling equation (85), the control law is redesigned and becomes:

$$u = -\varrho \text{sgn}(\hat{\sigma}(t)) \,, \quad \varrho > 0 \,, \tag{90}$$

$$\hat{\sigma}(t) = \zeta_1(t) + l_0 \zeta_0(t) \,, \tag{91}$$

where $\hat{\sigma}(t)$ is an estimate for $\sigma(t)$, using (88) and (89).

In the presented simulations, the controller (90)–(91) was implemented with $\varrho = 100$, $l_0 = 1$ [min^{-1}] and with estimated variables ζ_0 and ζ_1 given by (88)–(89). As for the unit of ϱ, it should be mentioned that this constant is measured in [μUmin /mg] during the positive control action; and it is measured in [pg/dL] during the negative control action.

Next, the simulation results are presented for the first-order sliding mode controller. Figure 6(a) illustrates the ability of the controller to safely regulate the blood glucose and avoid hypoglycemic and hyperglycemic episodes over the period assessed. Figure 6(b) will be discussed later on.

Figure 7(a) and Figure 7(b) demonstrate the role of bihormonal actuator, detaching the positive control action, u^+, and the negative control action, u^-, in two isolated and independent actions. The positive control action stands for insulin injection in the organism of the patient with T1DM, while the negative control action represents glucagon injection.

Since the control action can be understood as the union of the negative and the positive control actions, we may conclude that Figure 7 depicts the control action, which is notably discontinuous and counts with the presence of chattering. The high amplitude of the control action should be highlighted. This amplitude is due to the fact that the controller gains in (90) are extremely elevated. The consequence of it is the use of a large amount of hormones being injected in the patient every time. This effect is undesirable, since it may cause harm to the patient's health.

Figure 8(a) and Figure 8(b) attest in favour of the transient briefness of variables ζ_0 and ζ_1. In other words, within a short period of time, the estimates of the error, e, and its first derivative, $\dot{e}$, are perfectly obtained. Therefore, an estimate of the ideal sliding variable σ can be constructed from $\hat{\sigma}$, which in turn guarantees that the ideal sliding mode

$\sigma = 0$ is reached in finite time. Once again, it is noteworthy that the signals illustrated in Figure 8(a) are measured in [mg/dL], whilst the signals represented in Figure 8(b) are measured in [mg dL^{-1} min^{-1}].

As mentioned in Section 1.5, the meals made by the patient with T1DM are scheduled for 5:00, 12:00 and 18:00. As it is clear for the Figure 6(a), it is noted that in the instants when the patient makes his meals, oscillations appear in the glycemic curve. Indeed, there is a forward relation between feeding, $d(t)$, and the glycemic curve, $x_1(t)$. Next, this relationship will be elucidated in the light of control theory.

Note that during the controller design, the variable $d(t)$ was assumed to be uniformly upper bounded except for a zero measure set in the sense of Lebesgue. It was also discussed the double interpretation that could be made from this variable: from the medical point of view, it represents the effects that feeding has over the patient's glycaemic curve; from the control point of view, it represents an unmatched disturbance.

Although any demonstration had been presented, it was said that, in face of a case of unmatched disturbance, it was necessary that both the differentiator gain, C, and the modulation function of the controller, ϱ, must be capable of upper bound the disturbance, $d(t)$, and its first derivative, $\dot{d}(t)$. This is a condition that must necessarily be met in order for the differentiator to be able to provide ζ_1, where ζ_1 is the estimate of the derivative of the tracking error. It was said that the knowledge of this variable was necessary to the construction of the sliding surface $\sigma = 0$.

Notice, however, that if the disturbance $d(t)$ is mathematically represented by (39),it is easy to demonstrate that $\dot{d}(t)$ is described by a series of three impulses positioned in the same instants in which the meals are made. As known, the amplitude of an impulse is infinite. In this sense, it is important to highlight that neither the differentiator gain, either the modulation function of the controller are capable of upper bound the amplitude of $\dot{d}(t)$ in the instants that occur right after each one of the daily meals.

For this reason, precisely in these moments, it is evident that the construction of the sliding surface, $\sigma = 0$, is not possible, as depicted in Figure 6(b). Finally, a last comment should be made about this Figure: the variable $\hat{\sigma} = 0$ is measured in [mg dl^{-1} min^{-1}].

The simulation results concerning to the rest of the controllers will present a great deal of similarities with the results that were discussed in this section. For this reason, in

order to avoid the repetition of content, the next sections will provide shorter comments, always made in reference of the aforementioned ones.

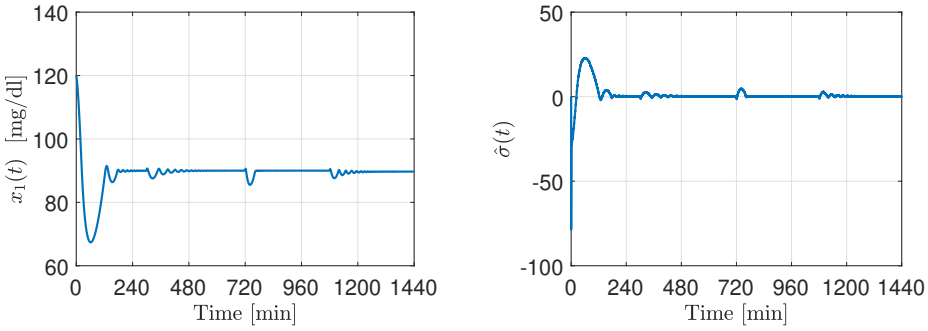

(a) Blood glucose concentration. (b) Sliding variable estimate $\hat{\sigma}$.

Figure 6: Sliding surface and glycaemia.

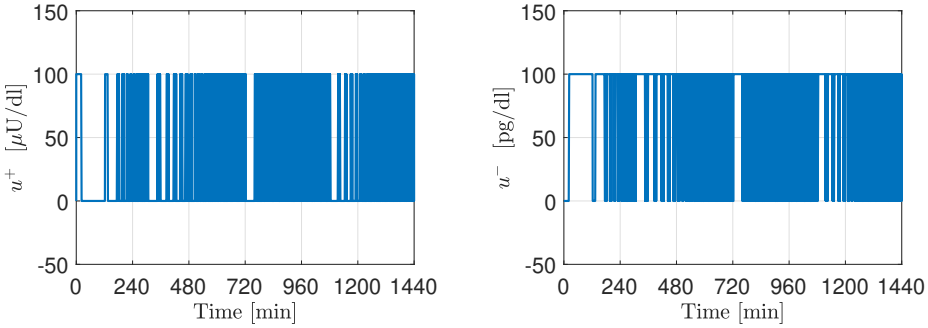

(a) Plasma insulin concentration. (b) Plasma glucagon concentration.

Figure 7: Control signals: Insulin and Glucagon.

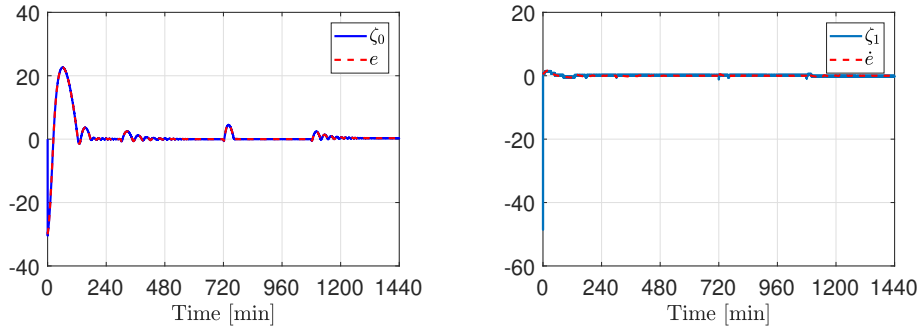

(a) Comparison between ζ_0 and e. (b) Comparison between ζ_1 and $\dot{e}$.

Figure 8: Exact differentiator.

1.10.2 Continuous FOSMC with Estimate of Sliding Variable Using Exact Differentiator and *Boundary Layer*

The major disadvantage of a classic sliding mode control strategy is the so called chattering effect. This phenomenon is characterized by small oscillations in the system output that may impair the performance of the control system. The chattering effect may arise due to unmodeled high-frequency dynamics, or due to digital implementation problems. However, the chattering effects can be reduced by the implementation of the technique described in Section 1.7.1: the Boundary Layer [35].

As it is noticed from Figure 9(b), the chattering effect has been alleviated from the control action $u(t)$ defined in (66). In other words, the control action now is described by a soft function, different from the discontinuous control action evidenced in the Section 1.10.1. This is due to the use of *boundary layer*. In the other aspects, the same one that was commented on in the Section 1.10.1 stands out.

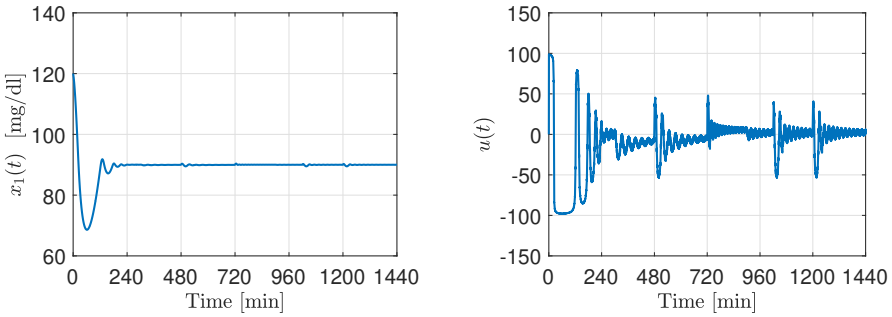

(a) Blood glucose concentration. (b) Controller action.

Figure 9: Glycaemia and Control Action.

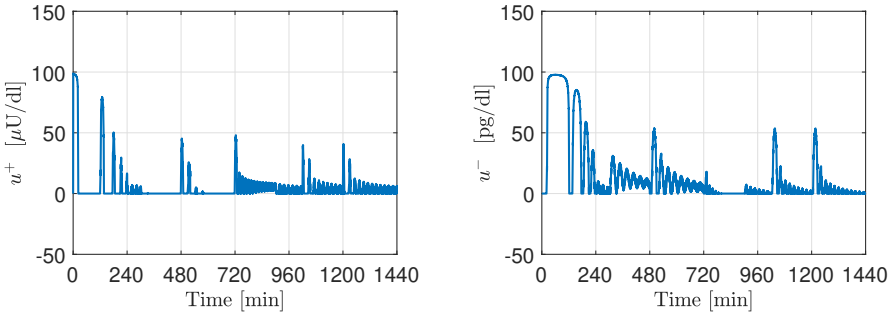

(a) Plasma insulin concentration. (b) Plasma glucagon concentration.

Figure 10: Control signals: Insulin and Glucagon.

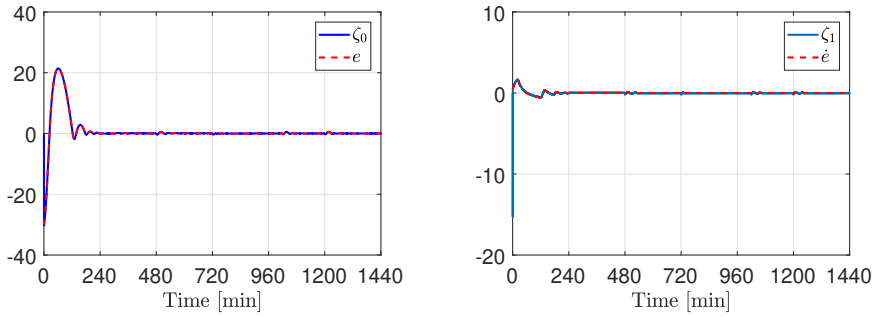

(a) Comparison between ζ_0 and e. (b) Comparison between ζ_1 and $\dot{e}$.

Figure 11: Exact Differentiator.

1.10.3 Discontinuous Non-singular Terminal Sliding Mode Control

Figure 12, Figure 13 and Figure 14 depict the simulation results obtained through Discontinuous Non-singular Terminal Sliding Mode Control.

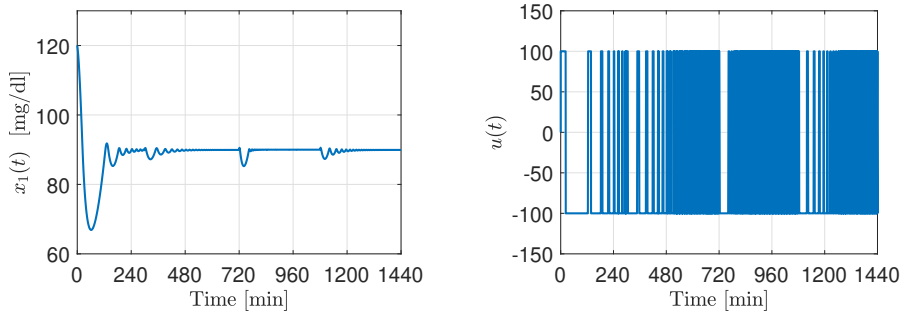

(a) Blood glucose concentration. (b) Controller action.

Figure 12: Curves related to Discontinuous Non-singular Terminal Sliding Mode Control.

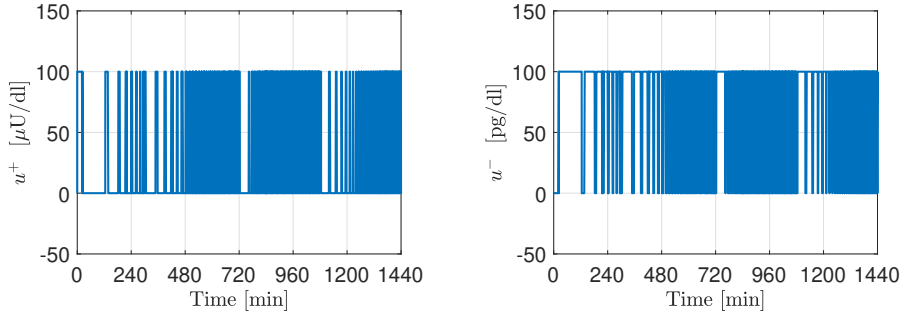

(a) Plasma insulin concentration. (b) Plasma glucagon concentration.

Figure 13: Curves related to Discontinuous Non-singular Terminal Sliding Mode Control.

In what concerns the Non-Singular Terminal Sliding Mode Controller, Figure 12(a) illustrates the ability of the controller to safely regulate the blood glucose and avoid

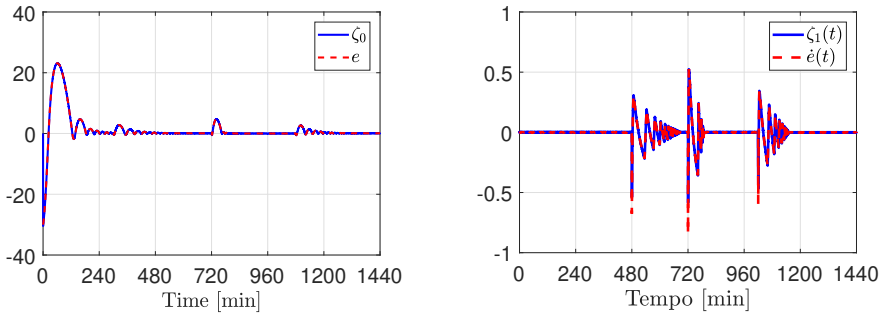

(a) Comparison between ζ_0 and e. (b) Comparison between ζ_1 and $\dot{e}$.

Figure 14: Curves related to Discontinuous Non-singular Terminal Sliding Mode Control.

hypoglycemic and hyperglycemic episodes over the period assessed.

As is evident from Figure 12(b), the discontinuous control action is affected by constant and high amplitude chattering. Once again, such amplitude is due to the high controller gains presented in (67). As a consequence, the blood glucose regulation is afforded, provided a large amount of hormone be injected in the patients bloodstream in the course of the day. Such effect, obviously, is not desirable, since it entails a plenty of risks to these patients health.

Figure 13(a) and Figure 13(b) portray the role of bihormonal actuator, detaching the positive control action, u^+, and the negative control action, u^-, in two independent and isolated signals. The positive control action represents insulin injection in T1DM subject, whilst negative control action stands for glucagon.

Figure 14(a) and Figure 14(b) attest in favour of the transient briefness of variables ζ_0 and ζ_1. Therefore, the ideal sliding variable σ can be constructed from $\hat{\sigma}$, which in turn guarantees that the ideal sliding mode $\sigma = 0$ is reached. Once again, it is noteworthy that the signals illustrated in Figure 14(a) are measured in [mg/dL], whilst the signals represented in Figure 14(b) are measured in $[\text{mg dL}^{-1} \text{ min}^{-1}]$.

1.10.4 Continuous Non-Singular Terminal Sliding Mode Control

In order to mitigate the chattering effect and reduce the amount of hormone injected into the patients' bloodstream, one possibility is to apply the continuous version of NSTSMC, the so called Continuous Non-singular Terminal Sliding Mode Algorithm (CNTSMA) [82]. The control action of the CNTSMA was defined in (83).

In Figure 15–Figure 17, the simulation results are presented for the continuous non-singular terminal sliding mode controller.

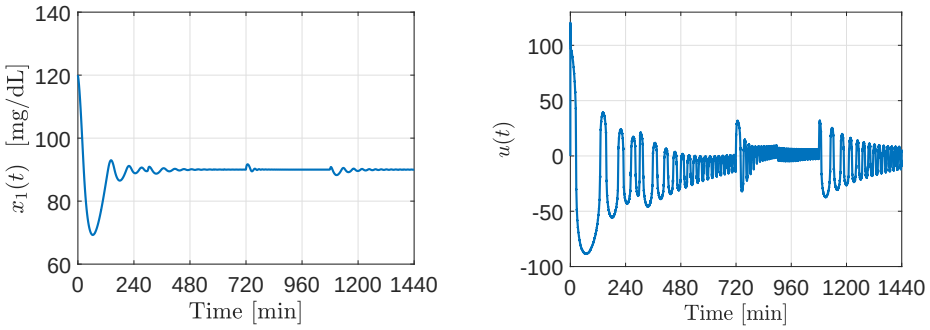

(a) Blood glucose concentration. (b) Controller action.

Figure 15: Control action and glycaemia.

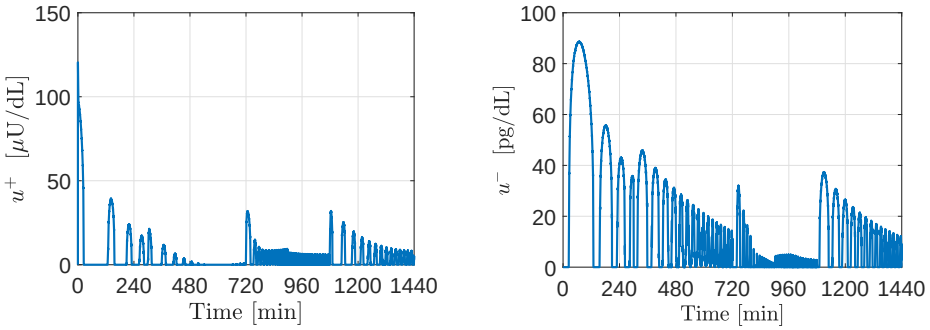

(a) Plasma insulin concentration. (b) Plasma glucagon concentration.

Figure 16: Control signals: Insulin and Glucagon.

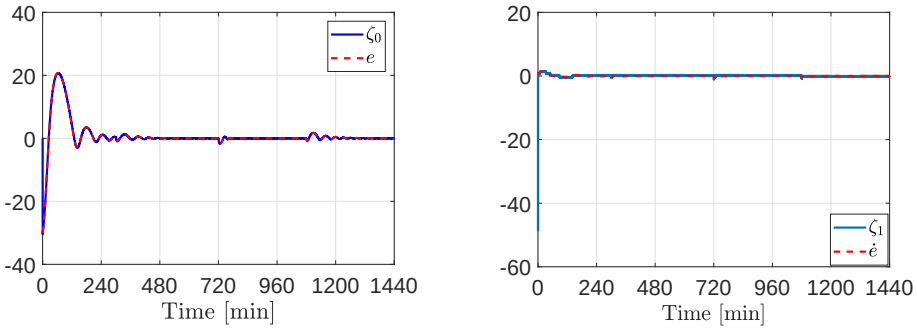

(a) Comparison between ζ_0 and e. (b) Comparison between ζ_1 and $\dot{e}$.

Figure 17: Exact differentiator.

As can be seen from Figure 15(b), the chattering effect was alleviated from the control action $u(t)$. In other words, the control action is now described by a smooth

function, while the control action provided in Section 1.10.3 was discontinuous. Moreover, Figure 16 depicts also that the control action has a variable amplitude. In the remaining aspects, the issues that are to be underscored here are not different from those presented in the Section 1.10.1.

2 GLOBAL STABILIZATION FOR A CLASS OF HYPERCHAOTIC SYSTEMS BY CASCADE NORM OBSERVERS WITH APPLICATION TO SECURE COMMUNICATION

2.1 Introduction

Chaos and control theory have been applied to a plenty of fields: electronic circuits [83], stabilization [84], synchronization [85], safe communication [86], energy conversion [87], meteorology [88],targeting [89] and neuroscience [90].

In [91, 92], adaptive and sliding mode control laws have been applied to Chua's circuit [93], while *backstepping* and variable structure approaches were proposed in [94,95] to stabilize the Lorenz's system in the presence of disturbances. On the other hand, sliding mode controllers have been designed to stabilize Liu's chaotic circuit in [96–98] and Genesio's third–order chaotic system in [99]. Hyperchaos synchronization was proposed in [100] via modified adaptive sliding mode control.

In all the mentioned works [91–100], the full-state measurement was necessary and/or only the local stability could be proved. Most of the existing literature about nonlinear control theory is based on the knowledge of the system state vector. Nevertheless, this condition is not always met in practice. In general, the full-state vector is not measured due to sensor limitations of localization and quantity. Thus, the unmeasured variables are not physically or economically available.

In this sense, output-feedback strategy presents itself as an interesting approach. In [101] and [102], applications to security communication systems were presented, and the synchronization of chaotic systems was achieved by using output-feedback sliding mode control. Besides, in both articles, the cryptography is implemented through a conventional method called *two-channel transmission*. The technique of the two-channel transmission has been proposed in [103].

The contribution of this manuscript is the proposal of a new control strategy to globally stabilize a class of hyperchaotic systems using sliding mode control [104]. It has been discovered that the considered seventh order dimension hyperchaotic system possesses an ISS property which allows the design of a global controller using only input/output information. The term ISS means Input-to-State Stability (or Stable, according to the context) as usually defined in [76]. It is noteworth that the ISS concept is the baseline of

the stability proof that is about to be presented in this chapter.

Instead of applying standard observers, we have used norm observers in cascade to construct a norm bound for the unmeasured state vector in the proposed output-feedback scheme. Such estimators are more robust to uncertainties, offering upper bounds to the state norm. In addition, the developed controller is applied to secure communication, where the fast synchronization and indirect encryption based on the concepts of sliding modes, equivalent and average control are the major ingredients of the proposed recipe. Here, the term *indirect* refers to the fact that the message is not directly send to the receiver device. The reconstruction process is based on sliding mode equivalent control theory.

At last, it is worth mentioning that the control strategy presented here can be applied to a wide class of hyperchaotic systems in order to guarantee *global stability properties* by using only *output feedback*, as discussed in the conclusions.

2.2 Seventh Dimension Hyperchaotic System

This work considers the stabilization problem for the following hyperchaotic system [105] [7]:

$$\dot{x}_1(t) = -15x_1(t) + 15x_5(t) - 5x_5(t)x_6(t)x_7(t)\,, \tag{92}$$

$$\dot{x}_2(t) = -0.5x_2(t) - 25x_6(t) + x_1(t)x_6(t)x_7(t)\,, \tag{93}$$

$$\dot{x}_3(t) = -15x_3(t) + 15x_5(t) - 0.1x_1(t)x_2(t)x_7(t)\,, \tag{94}$$

$$\dot{x}_4(t) = -15x_4(t) + 10x_1(t) - x_1(t)x_2(t)x_3(t)\,, \tag{95}$$

$$\begin{aligned}\dot{x}_5(t) = &-15x_5(t) + 10x_7(t) - x_2(t)x_3(t)x_4(t) \\ &+ d_u(t) + u(t)\,,\end{aligned} \tag{96}$$

$$\dot{x}_6(t) = -10x_6(t) + 10x_5(t) + x_2(t)x_3(t)x_5(t)\,, \tag{97}$$

$$\dot{x}_7(t) = -5x_7(t) + 4x_2(t) - 1.5x_1(t)x_5(t)x_6(t)\,, \tag{98}$$

$$\begin{aligned}y(t) &= [y_1(t)\ y_2(t)\ y_3(t)]^T \\ &:= [x_5(t)\ x_6(t)\ x_7(t)]^T\,,\end{aligned} \tag{99}$$

[7] However, the same control strategy proposed here could have been used to stabilize a class of chaotic and hyperchatic systems, such as those described in Table 2.

where the state vector is $x := [x_1\ x_2\ x_3\ x_4\ x_5\ x_6\ x_7]^T \in \mathbb{R}^7$, $u \in \mathbb{R}$ is the control signal, $y \in \mathbb{R}^3$ is the measured output vector. The input disturbance $d_u(t) \in \mathbb{R}$ is piecewise continuous and unknown. However, an upper bound $\bar{d}_u(t)$ is known such that

$$|d_u(t)| \leq \bar{d}_u(t) \leq \bar{d}_{\text{sup}} < +\infty, \forall t \geq 0\,. \tag{100}$$

The solution of this set of differential equations is a vector function $x(t)$ ($\forall t \geq 0$) which satisfies (92)–(98) to a given initial condition $x(0) \in \mathbb{R}^7$. Filippov's definition [106] for the solution of discontinuous differential equations is assumed throughout the paper, since the input $u(t)$ is a switching based control signal to be defined later on. In order to avoid clutter, the symbol u alone, without the argument t, represents a switching control law which is not an usual function of t when sliding mode takes place. On the other hand, we denote the extended equivalent control by $u(t)$ (instead of $u_{eq}(t)$) which, by definition, is piece-wise continuous. Note that u can always be replaced by $u(t)$ in the right-hand side of the differential equations.

It is noteworthy that the reason why the output variables are chosen as $y := [\ x_5\ x_6\ x_7]^T$ is that by doing so, it is possible to use equations (96)-(98) to construct the cascade norm observers necessary to estimate the unknown portion of the state vector. Moreover, the control action is chosen to be in the ODE that describes the x_5 dynamic because by doing so, the output variable x_5 has unitary relative degree, what makes the project of the controller simpler, since it does not require the derivatives of the output signal.

Figure 18 presents some of the state variables from the system (92)–(98). The initial condition chosen is $x(0) = [\ 0\ 1\ 0\ 1\ 0\ 1\ 0]^T$. Its chaotic behavior is illustrated to the case where there is no control action being applied and the system is free of disturbances.

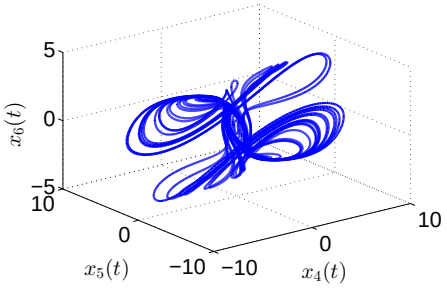

Figure 18: Trajectory of the state variables x_4, x_5 and x_6 for the hyperchaotic system (92)–(98) with $u(t) \equiv 0$ and $d_u(t) \equiv 0$.

2.3 Cascade Norm Observers

The norm observer is a tool which allows to estimate an upper bound to the norm of each system state variable. This is performed by means of the upper bounds of the system parameters and the available state variables. This section was based on [107].

For instance, consider a scalar uncertain nonlinear system described by:

$$\dot{x}(t) = \alpha x(t) + \beta z(t) + \gamma q(t) r(t) s(t)\,, \tag{101}$$

where $q \in \mathbb{R}$, $r \in \mathbb{R}$, $s \in \mathbb{R}$ and $z \in \mathbb{R}$ are input signals and $x \in \mathbb{R}$ is the unmeasured state variable. We assume that the parameters are uncertain such that $\alpha \in \mathbb{R}^-$, $\beta \in \mathbb{R}$ and $\gamma \in \mathbb{R}$, with known upper bounds satisfying

$$\bar{\alpha} \geq \alpha, \quad \bar{\beta} \geq |\beta| \quad \text{e} \quad \bar{\gamma} \geq |\gamma|\,. \tag{102}$$

The description of a norm observer for an unmeasured variable depends on the amount of available inputs. When all the system inputs in (101) are known, the norm observer is a dynamic system which can be described by:

$$\dot{\hat{x}}(t) = \bar{\alpha}\hat{x}(t) + \bar{\beta}|z(t)| + \bar{\gamma}|q(t)||r(t)||s(t)|\,. \tag{103}$$

If only one of the inputs is unknown, namely $q(t)$, it is necessary to know the respective state-norm estimate $\hat{q}(t)$ for it. Thus, applying the Young's inequality [76], p.395, in equation (103), the norm observer to the system (101) can be obtained as

$$\dot{\hat{x}}(t) = \bar{\alpha}\hat{x}(t) + \bar{\beta}|z(t)| + \frac{\bar{\gamma}}{\mu}|\hat{q}(t)|^p + \bar{\gamma}\mu^{\frac{1}{p-1}}(|r(t)||s(t)|)^{\frac{p}{p-1}}\,. \tag{104}$$

In case of two or more entrances are unknown, it is necessary that the respective observers to be available. Suppose all the inputs q, r, s and z are unavailable. In this case, the Young's inequality must be recursively applied in equation (103) so that the norm observer to the system (101) can be constructed by cascading the norm estimates of the unknown

inputs as follows

$$\dot{\hat{x}}(t) = \bar{\alpha}\hat{x}(t) + \bar{\beta}|\hat{z}(t)| + \frac{\bar{\gamma}}{\mu}|\hat{q}(t)|^p + \bar{\gamma}\mu^{\frac{2-p}{p-1}}|\hat{r}(t)|^{\frac{p^2}{p-1}} + \bar{\gamma}\mu^{\frac{2}{p-1}}|\hat{s}(t)|^{\left(\frac{p}{p-1}\right)^2}, \tag{105}$$

where $\hat{q} \in \mathbb{R}$, $\hat{r} \in \mathbb{R}$, $\hat{s} \in \mathbb{R}$ and $\hat{z} \in \mathbb{R}$ are the norm-estimate variables and the parameters μ and p came from the application of the Young's inequality.

Definition 1. *The Young's inequality [76], p.395, is given by:*

$$vw \leq \frac{1}{\mu}v^p + \mu^{\frac{1}{p-1}}\ w^{\frac{p}{p-1}}$$

valid $\forall\ v \geq 0,\ w \geq 0,\ \mu > 0$ *and* $p > 1$.

The following lemma describes how to obtain the norm observers (103)–(105) for the dynamic system (101).

Lemma 1. *Consider the scalar nonlinear system (101) with state variable* $x \in \mathbb{R}$ *and the norm observers candidates (103)–(105), with state variable* $\hat{x} \in \mathbb{R}$ *and input signals* $q \in \mathbb{R}$, $r \in \mathbb{R}$, $s \in \mathbb{R}$, $z \in \mathbb{R}$. *If* $\bar{\alpha}$, $\bar{\beta}$ *and* $\bar{\gamma}$ *are upper bounds to the parameters* α, β *and* γ *satisfying the inequalities (102), then the absolute value of the state variable* x *satisfies:*

$$|x(t)| \leq \hat{x}(t) + \mathrm{e}^{\bar{\alpha}t}\left(|x(0)| + |\hat{x}(0)|\right), \quad \forall t \geq 0\,. \tag{106}$$

Proof 3.: *Define the quadratic function* $V := x^2$. *From the differential equation (101) and the upper bounds in (102), it can be concluded the time-derivative of* V *satisfies*

$$\begin{aligned}
\dot{V} &= 2x(\alpha x + \beta z + \gamma qrs) \\
&= 2(\alpha x^2 + \beta xz + \gamma qrsx) \\
&\leq 2(\alpha|x|^2 + |\beta||x||z| + |\gamma||q||r||s||x|) \\
&\leq 2(\bar{\alpha}|x|^2 + \bar{\beta}|x||z| + \bar{\gamma}|q||r||s||x|) \\
&= 2|x|(\bar{\alpha}|x| + \bar{\beta}|z| + \bar{\gamma}|q||r||s|)\,.
\end{aligned} \tag{107}$$

Using the Young's inequality, we have

$$\dot{V} \leq 2|x| \ (\bar{\alpha}|x| + \bar{\beta}|z| + \frac{\bar{\gamma}}{\mu}|q|^p + \bar{\gamma}\mu^{\frac{1}{p-1}}(|r||s|)^{\frac{p}{p-1}}) \,, \tag{108}$$

and applying the Young's inequality once again, one can write

$$\begin{aligned} \dot{V} \leq 2|x|\Big(\bar{\alpha}|x| + \bar{\beta}|z| + \frac{\bar{\gamma}}{\mu}|q|^p + \bar{\gamma}\mu^{\frac{2-p}{p-1}}|r|^{\frac{p^2}{p-1}} \\ + \bar{\gamma}\mu^{\frac{2}{p-1}}|s|^{\left(\frac{p}{p-1}\right)^2}\Big) \,. \end{aligned} \tag{109}$$

Now, defining

$$\tilde{x} := \sqrt{V} = |x| \,, \tag{110}$$

the inequality (107) can be rewritten as

$$\dot{\tilde{x}} \leq \bar{\alpha}\tilde{x} + \bar{\beta}|z| + \bar{\gamma}|q||r||s| \,, \quad \forall t \geq 0 \,. \tag{111}$$

From the Comparison Lemma [76], pp.84-87, an upper bound $\bar{x}$ for $\tilde{x}$ is the solution of the differential equation

$$\dot{\bar{x}} = \bar{\alpha}\tilde{x} + \bar{\beta}|z| + \bar{\gamma}|q||r||s| \,, \quad \forall t \geq 0 \,, \tag{112}$$

provides the initial condition $\bar{x}(0) = \tilde{x}(0) \geq 0$. The solution of the differential equation (112) is given by

$$\bar{x}(t) = \mathrm{e}^{\bar{\alpha}t}\bar{x}(0) + \mathrm{e}^{\bar{\alpha}t} * (\bar{\beta}|z| + \bar{\gamma}|q||r||s|) \,, \quad t \geq 0 \,, \tag{113}$$

which is an upper bound for $|x(t)|$, where $\bar{x}(0) = |x(0)|$ and $*$ denotes the convolution operator. On the other hand, the solution of the differential equation of the norm observer (103) is given by

$$\hat{x}(t) = \mathrm{e}^{\bar{\alpha}t}\hat{x}(0) + \mathrm{e}^{\bar{\alpha}t} * (\bar{\beta}|z| + \bar{\gamma}|q||r||s|) \,, \quad t \geq 0 \,. \tag{114}$$

By subtracting (113) from (114), we have

$$\bar{x}(t) - \hat{x}(t) = \mathrm{e}^{\bar{\alpha}t} \left(|x(0)| - \hat{x}(0)\right) \,, \quad t \geq 0 \,. \tag{115}$$

Finally, since $|x(t)| \leq \bar{x}(t)$, the inequality (106) holds, with $\hat{x}(t)$ governed by (103). The process to obtain the norm observer from inequalities (108) and (109) is analogous to the one done for (107). The observers described by equations (104) and (105) satisfy (115) since $\hat{q}$, $\hat{r}$ and $\hat{s}$ are at least norm bounds for q, r and s, respectively. Therefore, in all these cases, (106) is also verified.

If the parameter $\bar{\alpha} < 0$, then the state-norm observers (103)–(105) and, consequently, the linear time-variant system (101) are ISS. The concept of minimum phase to linear time-invariant system can be generalized to nonlinear systems assuming that the zero dynamics (112) is stable.

Using Lemma 1, the dynamic equation that governs the norm observer for (1) with norm estimate $\hat{x}_1$ follows the same steps taken to obtain (103). The norm observer $\hat{x}_2$ falls in the case described by the equation (104). At last, the norm observers with norm bounds $\hat{x}_3$ and $\hat{x}_4$ for x_3 and x_4 are referred to (105). Thereby, it is possible to obtain the following cascade norm observers for the subsystem (92)–(95) from the measurable signals x_5, x_6 and x_7:

$$\dot{\hat{x}}_1 = \bar{\alpha}_1\hat{x}_1 + \bar{\beta}_1|x_5| + \bar{\gamma}_1|x_5||x_6||x_7| \tag{116}$$

$$\dot{\hat{x}}_2 = \bar{\alpha}_2\hat{x}_2 + \bar{\beta}_2|x_6| + \frac{\bar{\gamma}_2}{\mu_2}|\hat{x}_1|^{p_2} + \bar{\gamma}_2\mu_2^{\frac{1}{p_2-1}}(|x_6||x_7|)^{\frac{p_2}{p_2-1}} \tag{117}$$

$$\dot{\hat{x}}_3 = \bar{\alpha}_3\hat{x}_3 + \bar{\beta}_3|x_5| + \frac{\bar{\gamma}_3}{\mu_3}|\hat{x}_2|^{p_3} + \bar{\gamma}_3\mu_3^{\frac{2-p_3}{p_3-1}}|\hat{x}_1|^{\frac{p_3^2}{p_3-1}} + \bar{\gamma}_3\mu_3^{\frac{2}{p_3-1}}|x_7|^{\left(\frac{p_3}{p_3-1}\right)^2} \tag{118}$$

$$\dot{\hat{x}}_4 = \bar{\alpha}_4\hat{x}_4 + \bar{\beta}_4|\hat{x}_1| + \frac{\bar{\gamma}_4}{\mu_4}|\hat{x}_3|^{p_4} + \bar{\gamma}_4\mu_4^{\frac{2-p_4}{p_4-1}}|\hat{x}_1|^{\frac{p_4^2}{p_4-1}} + \bar{\gamma}_4\mu_4^{\frac{2}{p_4-1}}|\hat{x}_2|^{\left(\frac{p_4}{p_4-1}\right)^2}, \tag{119}$$

where $-15 \leq \bar{\alpha}_1 < 0$, $-0.5 \leq \bar{\alpha}_2 < 0$, $-15 \leq \bar{\alpha}_3 < 0$, $-15 \leq \bar{\alpha}_4 < 0$, $\bar{\beta}_1 \geq 15$, $\bar{\beta}_2 \geq 25$, $\bar{\beta}_3 \geq 15$, $\bar{\beta}_4 \geq 10$, $\bar{\gamma}_1 \geq 5$, $\bar{\gamma}_2 \geq 1$, $\bar{\gamma}_3 \geq 1$, $\bar{\gamma}_4 \geq 1$, $p_2 > 1$, $p_3 > 1$, $p_4 > 1$, $\mu_2 > 0$, $\mu_3 > 0$ and $\mu_4 > 0$.

2.4 Stabilization via Output Feedback

For the controller design, the output vector y is described by $y = [y_1\ y_2\ y_3]^T = [x_5\ x_6\ x_7]^T$. In addition, the control signal u has been injected into the fifth differential equation (96). These choices were motivated by the need to ensure the ISS properties in order to construct the norm observers for the following state variables: x_1, x_2, x_3 and x_4. Moreover, this input-output selection restricts the control problem to the case of

relative degree one [76]. The unitary relative degree facilitates the design of a sliding mode controller via output feedback, making it amenable by pure Lyapunov function.

Theorem 3. *Consider the hyperchaotic system described by (92)–(99) and the norm observers (116)–(119). If the following sliding mode control law via output feedback is applied*

$$u = -\rho(t)\,\mathrm{sgn}(x_5(t))\,, \tag{120}$$

with modulation function ρ satisfying

$$\rho(t) = \bar{\alpha}_5|x_5| + \bar{\beta}_5|x_7| + \bar{\gamma}_5|\hat{x}_2||\hat{x}_3||\hat{x}_4| + \bar{d}_u(t) + \delta, \tag{121}$$

where $\delta > 0$ is any arbitrary constant and $|d_u(t)| \leq \bar{d}_u(t)$, $\forall t \geq 0$, then the ideal sliding mode $y_1 = x_5 = 0$ occurs in finite time. Moreover, the equilibrium point of the closed-loop system

$$[x_1\ x_2\ x_3\ x_4\ x_5\ x_6\ x_7\ \hat{x}_1\ \hat{x}_2\ \hat{x}_3\ \hat{x}_4]^T = [0\ 0\ \cdots\ 0\ 0]^T$$

is globally asymptotically stable.

Proof 4.*: From Lemma 1, the state variable x_i can be majorized by*

$$|x_i(t)| \leq \hat{x}_i(t) + \pi_i(t)\,, \quad \forall t \geq 0\,, \tag{122}$$

where $i = 1, 2, 3$ and 4; $\hat{x}_i(t)$ is the norm observer state and $\pi_i(t) = \mathrm{e}^{\bar{\alpha}_i t}\left(|x_i(0)| + |\hat{x}_i(0)|\right)$ decays exponentially. Consider the following Lyapunov function candidate

$$V = \frac{1}{2}{x_5}^2\,, \tag{123}$$

with time-derivative $\dot{V} = x_5\dot{x_5}$. *Hence,*

$$\begin{aligned}
\dot{V} &= x_5\dot{x_5} \\
&= x_5[-15x_5 + 10x_7 - x_2x_3x_4 + d_u + u] \\
&= -15x_5^2 + 10x_5x_7 - x_2x_3x_4x_5 + x_5d_u - \rho x_5\mathrm{sgn}(x_5) \\
&\leq \bar{\alpha}_5|x_5|^2 + \bar{\beta}_5|x_5||x_7| + \bar{\gamma}_5|x_2||x_3||x_4||x_5| \\
&\quad + |x_5||d_u| - \rho|x_5| \\
&\leq |x_5|\Big(\bar{\alpha}_5|x_5| + \bar{\beta}_5|x_7| + \bar{\gamma}_5|\hat{x}_2 + \pi_2||\hat{x}_3 \\
&\quad + \pi_3||\hat{x}_4 + \pi_4| + \bar{d}_u - \rho\Big) \\
&\leq |x_5|\Big(\bar{\alpha}_5|x_5| + \bar{\beta}_5|x_7| + \bar{\gamma}_5|\hat{x}_2||\hat{x}_3||\hat{x}_4| + |\hat{x}_2||\hat{x}_3|\pi_4 \\
&\quad + |\hat{x}_2||\hat{x}_4|\pi_3 + |\hat{x}_2|\pi_3\pi_4 + |\hat{x}_3||\hat{x}_4|\pi_2 + |\hat{x}_3|\pi_2\pi_4 \\
&\quad + |\hat{x}_4|\pi_2\pi_3 + \pi_2\pi_3\pi_4 + \bar{d}_u - \rho\Big)
\end{aligned} \tag{124}$$

Applying the Young's inequality, with $\mu = 1$ *and* $p = 2$, *into the terms multiplied by* π_i, *we have :*

$$\begin{aligned}
\dot{V} \leq & |x_5|\Big(\bar{\alpha}_5|x_5| + \bar{\beta}_5|x_7| + \bar{\gamma}_5|\hat{x}_2||\hat{x}_3||\hat{x}_4| + \hat{x}_2^2\hat{x}_3^2 + \pi_4^2 \\
& + \hat{x}_2^2\hat{x}_4^2 + \pi_3^2 + \hat{x}_2^2 + \pi_3^2\pi_4^2 + \hat{x}_3^2\hat{x}_4^2 + \pi_2^2 + \hat{x}_3^2 \\
& + \pi_2^2\pi_4^2 + \hat{x}_4^2 + \pi_2^2\pi_3^2 + \pi_2\pi_3\pi_4 + \bar{d}_u - \rho\Big) \\
\leq & |x_5|\Big(\bar{\alpha}_5|x_5| + \bar{\beta}_5|x_7| + \bar{\gamma}_5|\hat{x}_2||\hat{x}_3||\hat{x}_4| + \hat{x}_2^2\hat{x}_3^2 \\
& + \hat{x}_2^2\hat{x}_4^2 + \hat{x}_2^2 + \hat{x}_3^2\hat{x}_4^2 + \hat{x}_3^2 + \hat{x}_4^2 + \pi_2^2 + \pi_3^2 + \pi_4^2 \\
& + \pi_2^2\pi_3^2 + \pi_2^2\pi_4^2 + \pi_3^2\pi_4^2 + \pi_2\pi_3\pi_4 + \bar{d}_u - \rho\Big)
\end{aligned}$$

Therefore, using a modulation function that satisfies (121), it can be concluded that

$$\dot{V} \leq \left[-\delta + \Pi(t)\right]|y_1|\,, \quad t \geq 0\,, \tag{125}$$

where $\Pi(t) = \pi_2^2+\pi_3^2+\pi_4^2+\pi_2^2\pi_3^2+\pi_2^2\pi_4^2+\pi_3^2\pi_4^2+\pi_2\pi_3\pi_4$ *is a term which decays exponentially. It is possible to rewrite (125) with* $\tilde{y}_1(t) := \sqrt{2V} = |y_1(t)|$ *such that*

$$\dot{\tilde{y}}_1 \leq -\delta + \Pi(t)\,, \quad t \geq 0\,. \tag{126}$$

Using the Comparison Theorem [106], there exists an upper bound $\bar{y}_1(t)$ *for* $\tilde{y}_1(t)$ *satisfying the differential equation*

$$\dot{\bar{y}}_1 = -\delta + \Pi(t)\,, \quad \bar{y}_1(0) = \tilde{y}_1(0) \geq 0\,, \quad t \geq 0\,. \tag{127}$$

Integrating both sides of the above equation, we arrive at the solution

$$\bar{y}_1(t) - \bar{y}_1(0) = -\delta t + \int_0^t \Pi(\tau)d\tau \quad t \geq 0\,. \tag{128}$$

Since the function $\Pi(t)$ *is positive and decays exponentially, its integral converges to some constant which depends on the initial state, which is denoted by* $\mathscr{C}(x(0))$*. In this sense, the following inequality is valid:*

$$\begin{aligned}\bar{y}_1(t) &= -\delta t + \int_0^t \Pi(\tau)d\tau + \bar{y}_1(0) \\ &\leq -\delta t + \int_0^{+\infty} \Pi(\tau)d\tau + \bar{y}_1(0) \\ &= -\delta t + \mathscr{C}(x(0)) + \bar{y}_1(0)\,, \quad t \geq 0\,.\end{aligned} \tag{129}$$

Considering that $\bar{y}_1 \geq 0$ *is continuous, then* $\bar{y}_1(t)$ *becomes identically zero* $\forall t \geq t_1 = \delta^{-1}[\mathscr{C}(x(0)) + \bar{y}_1(0)]$*. Thus, it can be concluded that there exists a finite time* $0 < t_s \leq t_1$*, where the sliding mode starts such that* $y_1(t) = x_5 = 0$*,* $\forall t \geq t_s$*.*

It is well known that the chaotic orbits remain at least within a bounded region of the state space, even when $x_5 = 0$*, since the system (92)–(98) has two positive Lyapunov exponents [105]. It ensures the trajectories are confined in a compact set corresponding to the hyperchaotic atractor a priori. Therefore, the cross terms* $x_i x_j x_k$*, for* $i \neq j \neq k$*, disappear if one of the variables eventually converges to zero.*

Now, the stabilization result can be easily verified from equations (92)–(98). With x_5 *in sliding motion (*$x_5 = 0$*), it can be claimed that:* x_1 *and* x_6 *converge exponentially to zero because (92) and (97) are ISS with respect to* x_5*. Since the dynamics of* x_4 *in (95) is ISS with respect to* x_1*, so if* x_1 *converges to zero,* x_4 *decays exponentially. In the case of the state variable* x_2*, the ISS property of (97) is verified concerning the variable* x_6*. Since* x_6 *decays exponentially,* x_2 *goes to zero exponentially too. The subsystem that governs* x_7 *is ISS with respect to the inputs* x_2*,* x_4*,* x_5 *and* x_6*. Since all inputs converge to zero, thus*

x_7 decays exponentially. The state variable x_3 in (94) also decays exponentially, since x_1, x_2, x_5 and x_7 tend to zero. In a nutshell, it can be concluded that x_5 goes to zero by the direct action of the controller, while the other state variables of the hyperchaotic system converge exponentially, due to the ISS property of each one of the subsystems in (92)–(98).

Since the terms $\pi_1(t)$, $\pi_2(t)$, $\pi_3(t)$ and $\pi_4(t)$ converge asymptotically to zero as well as $x_1(t)$, ..., $x_7(t)$, then, we conclude that the state variables of the norm observers in (116)–(119), namely, $\hat{x}_1(t)$, $\hat{x}_2(t)$, $\hat{x}_3(t)$ and $\hat{x}_4(t)$, also converge asymptotically to zero by using inequality (122). □

2.5 Simulations

In the following simulation results for the hyperchaotic system (92)–(98), the parameters of the norm observer (116)–(119) have been chosen as $\bar{\alpha}_1 = -13$, $\bar{\beta}_1 = 20$, $\bar{\gamma}_1 = 10$, $\bar{\alpha}_2 = -0.5$, $\bar{\beta}_2 = 25$, $\bar{\gamma}_2 = 1$, $\bar{\alpha}_3 = -1$, $\bar{\beta}_3 = 16$, $\bar{\gamma}_3 = 0.15$, $\bar{\alpha}_4 = -14$, $\bar{\beta}_4 = 11$, $\bar{\gamma}_4 = 1.5$, $\mu_2 = \mu_3 = \mu_4 = 1$ and $p_2 = p_3 = p_4 = 2$.

The input disturbance in (96) is $d_u(t) = 0.02\cos(4t)$ and its upper bound used in the modulation signal ρ was $\bar{d}_u = 0.05$, so that was met the hypothesis that the disturbance d was uniformly bounded, as was said in equation (100). In addition, the parameter $\delta = 0.001$ was chosen to implement (120)–(121), where δ is a sufficiently small constant. The initial conditions are given by: $x_1(0) = -1$, $x_2(0) = 1$, $x_3(0) = -0.5$, $x_4(0) = 0.5$, $x_5(0) = 0$, $x_6(0) = -0.25$, $x_7(0) = 0.25$, $\hat{x}_1(0) = 0.5$ and $\hat{x}_2(0) = \hat{x}_3(0) = \hat{x}_4(0) = 1$.

Figure 19 and Figure 20 present the trajectories of $|x_1(t)|$ and its upperbound $\hat{x}_1(t)$ given by the norm observer (116) in open-loop and closed-loop operation modes, respectively. Similar curves can be obtained for the duos ($|x_2|$, $\hat{x}_2$), ($|x_3|$, $\hat{x}_3$) and ($|x_4|$, $\hat{x}_4$). As expected, the signal $\hat{x}_1(t)$ majorizes $|x_1(t)|$ after a short transient due to the system initial conditions.

Figure 21 and Figure 22 show the performance of the proposed output-feedback sliding mode controller (120)–(121). The state of the closed loop system is forced to reach the equilibrium point as shown in Figure 21.

In Table 2, it is shown a class of chaotic systems with ISS properties for which the methodology presented here can be directly applied. Moreover, it is presented the cascade norm observers and the required control laws for each case.

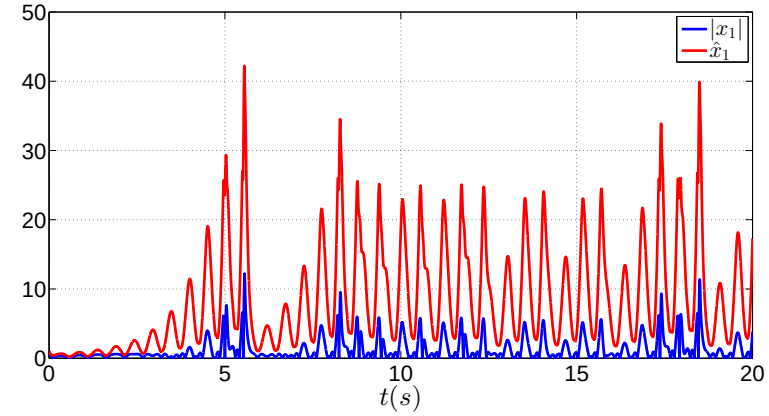

Figure 19: Open-loop system: $|x_1|$ and its upperbound $\hat{x}_1$.

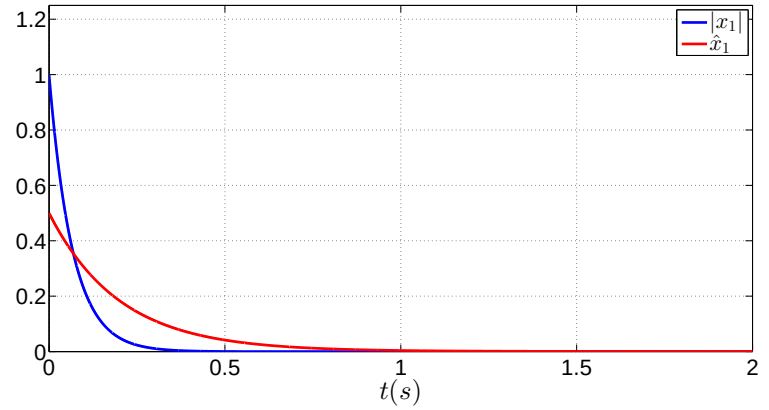

Figure 20: Closed-loop system: $|x_1|$ and its upperbound $\hat{x}_1$.

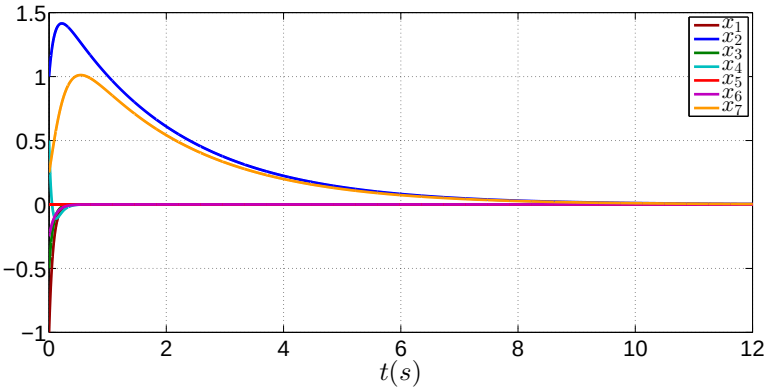

Figure 21: Convergence for the state variables of the controlled hyperchaotic system.

2.6 Synchronization Applied to Secure Communication via Equivalent/Average Control

Here, a strategy to synchronize two seven dimensional chaotic systems is presented. It is considered that only the output variables of each system (master and slave) are available. Norm observers are designed such that global stability properties of the closed-

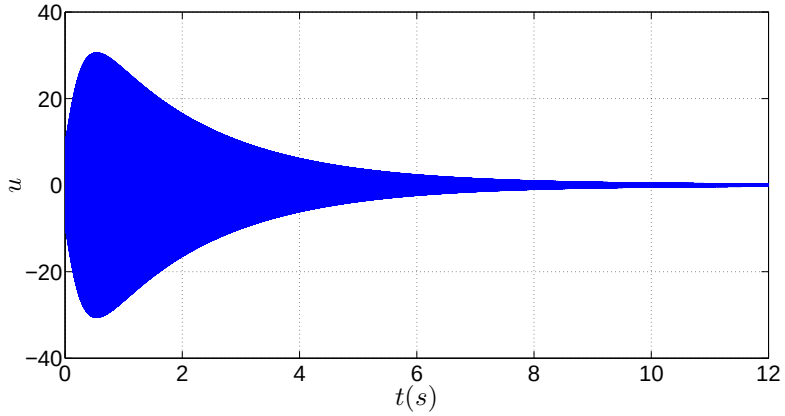

Figure 22: Control signal.

loop system are preserved. Moreover, it is worth to mention that syncronizing such chaotic systems is nothing but reaching the stabilization of the error dynamics. Therefore, the results presented in Section 2.4 are utilized here.

The chaotic transmitter dynamics is driven by

$$\dot{x}_{m1} = -15x_{m1} + 15x_{m5} - 5x_{m5}x_6x_{m7}\,, \tag{130}$$

$$\dot{x}_{m2} = -0.5x_{m2} - 25x_{m6} + x_{m1}x_{m6}x_{m7}\,, \tag{131}$$

$$\dot{x}_{m3} = -15x_{m3} + 15x_{m5} - 0.1x_{m1}x_{m2}x_{m7}\,, \tag{132}$$

$$\dot{x}_{m4} = -15x_{m4} + 10x_{m1} - x_{m1}x_{m2}x_{m3}\,, \tag{133}$$

$$\dot{x}_{m5} = -15x_{m5} + 10x_{m7} - x_{m2}x_{m3}x_{m4} + m\,, \tag{134}$$

$$\dot{x}_{m6} = -10x_{m6} + 10x_{m5} + x_{m2}x_{m3}x_{m5}\,, \tag{135}$$

$$\dot{x}_{m7} = -5x_{m7} + 4x_{m2} - 1.5x_{m1}x_{m5}x_{m6}\,, \tag{136}$$

$$y_m = [y_{m1}\ y_{m2}\ y_{m3}]^T := [x_{m5}\ x_{m6}\ x_{m7}]^T\,, \tag{137}$$

while in receptor, the dynamics is given by

$$\dot{x}_{s1} = -15x_{s1} + 15x_{s5} - 5x_{s5}x_{s6}x_{s7}\,, \tag{138}$$

$$\dot{x}_{s2} = -0.5x_{s2} - 25x_{s6} + x_{s1}x_{s6}x_{s7}\,, \tag{139}$$

$$\dot{x}_{s3} = -15x_{s3} + 15x_{s5} - 0.1x_{s1}x_{s2}x_{s7}\,, \tag{140}$$

$$\dot{x}_{s4} = -15x_{s4} + 10x_{s1} - x_{s1}x_{s2}x_{s3}\,, \tag{141}$$

$$\dot{x}_{s5} = -15x_{s5} + 10x_{s7} - x_{s2}x_{s3}x_{s4} + u_5\,, \tag{142}$$

$$\dot{x}_{s6} = -10x_{s6} + 10x_{s5} + x_{s2}x_{s3}x_{s5} + u_6\,, \tag{143}$$

$$\dot{x}_{s7} = -5x_{s7} + 4x_{s2} - 1.5x_{s1}x_{s5}x_{s6} + u_7\,, \tag{144}$$

$$y_s = [y_{s1}\ y_{s2}\ y_{s3}]^T := [x_{s5}\ x_{s6}\ x_{s7}]^T\,, \tag{145}$$

The error dynamics is defined as $e = x_s - x_m$, then

$$\begin{aligned}\dot{e}_1 = {} & -15e_1 + 15e_5 - 5e_5x_{s6}x_{s7} + 5x_{m5}e_6x_{s7} + \\ & + 5x_{m5}x_{m6}e_7\,,\end{aligned} \tag{146}$$

$$\begin{aligned}\dot{e}_2 = {} & -0.5e_2 - 25e_6 + e_1x_{s6}x_{s7} + 5x_{m1}e_6x_{s7} + \\ & + 5x_{m1}x_{m6}e_7\,,\end{aligned} \tag{147}$$

$$\begin{aligned}\dot{e}_3 = {} & -15e_3 + 15e_5 - 0.1e_1x_{s2}x_{s7} - 0.15x_{m1}e_2x_{s7} + \\ & - 0.1x_{m1}x_{m2}e_7\,,\end{aligned} \tag{148}$$

$$\begin{aligned}\dot{e}_4 = {} & -15e_4 + 10e_1 - e_1x_{s2}x_{s3} - x_{m1}e_2x_{s7} + \\ & - x_{m1}x_{m2}e_3\,,\end{aligned} \tag{149}$$

$$\begin{aligned}\dot{e}_5 = {} & -15e_5 + 10e_7 - e_2x_{s3}x_{s4} - x_{m2}e_3x_{s4} + \\ & - x_{m2}x_{m3}e_4 - m(t) + u_5\,,\end{aligned} \tag{150}$$

$$\begin{aligned}\dot{e}_6 = {} & -10e_5 + 10e_5 + e_2x_{s3}x_{s5} + x_{m2}e_3x_{s5} + \\ & + x_{m2}x_{m3}e_5 + u_6\,,\end{aligned} \tag{151}$$

$$\begin{aligned}\dot{e}_7 = {} & -5e_7 + 4e_2 - 1.5e_1x_{s5}x_{s6} - 1.5x_{m1}e_5x_{s6} + \\ & - 1.5x_{m1}x_{m5}e_6 + u_7\,.\end{aligned} \tag{152}$$

At this point, norm observers are applied in order to provide norm upper bounds

for the unmeasured state variables. The design follows the steps presented in Section 2.3. In this sense, upper bounds for the unmeasured master variables are obtained through

$$\dot{\hat{x}}_{m1} = -13.5\hat{x}_{m1} + 17.5|x_{m5}| + 6|x_{m5}x_{m6}x_{m7}|\,, \tag{153}$$

$$\dot{\hat{x}}_{m2} = -0.45\hat{x}_{m2} + 27.5|x_{m6}| + 1.1|\hat{x}_{m1}x_{m6}x_{m7}|\,, \tag{154}$$

$$\dot{\hat{x}}_{m3} = -13.5\hat{x}_{m3} + 11|x_{m5}| + 0.15|\hat{x}_{m1}\hat{x}_{m2}x_{m7}|\,, \tag{155}$$

$$\dot{\hat{x}}_{m4} = -13.5\hat{x}_{m4} + 11|\hat{x}_{m1}| + 1.1|\hat{x}_{m1}\hat{x}_{m2}\hat{x}_{m3}|\,, \tag{156}$$

and, for slave system,

$$\dot{\hat{x}}_{s1} = -13.5\hat{x}_{s1} + 17.5|x_{s5}| + 6|x_{s5}x_{s6}x_{s7}|\,, \tag{157}$$

$$\dot{\hat{x}}_{s2} = -0.45\hat{x}_{s2} + 27.5|x_{s6}| + 1.1|\hat{x}_{s1}x_{s6}x_{s7}|\,, \tag{158}$$

$$\dot{\hat{x}}_{s3} = -13.5\hat{x}_{s3} + 11|x_{s5}| + 0.15|\hat{x}_{s1}\hat{x}_{s2}x_{s7}|\,, \tag{159}$$

$$\dot{\hat{x}}_{s4} = -13.5\hat{x}_{s4} + 11|\hat{x}_{s1}| + 1.1|\hat{x}_{s1}\hat{x}_{s2}\hat{x}_{s3}|\,,. \tag{160}$$

Basically, the adopted strategy consists in driving the output error $y_e = [e_5\,,\ e_6\,,\ e_7]$ to zero in finite-time, so that the remaining error variables converge exponentially due to the system ISS properties [76]. Therefore, the inputs u_5, u_6 and u_7 are applied to equations (146), (147) and (152), respectively. When the system is in sliding mode ($e_5 \equiv 0$, $e_6 \equiv 0$ and $e_7 \equiv 0$) we can state that the error dynamics in (146)–(149) becomes

$$\dot{e}_1 = -15e_1, \tag{161}$$

$$\dot{e}_2 = -0.5e_2 + e_1x_{s6}x_{s7}, \tag{162}$$

$$\dot{e}_3 = -15e_3 - 0.1e_1x_{s2}x_{s7} - 0.15x_{m1}e_2x_{s7}\,, \tag{163}$$

$$\dot{e}_4 = -15e_4 + 10e_1 - e_1x_{s2}x_{s3} - x_{m1}e_2x_{s7} + \\ - x_{m1}x_{m2}e_3\,. \tag{164}$$

Thus, it is clear that the error variables e_1, e_2, e_3 and e_4 tend to zero exponentially due to ISS relationship with e_5, e_6 and e_7. In order to reach this condition, the following output-feedback control laws are applied:

$$u_5 = [17(|x_{s5}| + |x_{m5}|) + 12(|x_{s7}| + |x_{m7}|)+ \\ +|\hat{x}_{s2}\hat{x}_{s3}\hat{x}_{s4}| + |\hat{x}_{m2}\hat{x}_{m3}\hat{x}_{m4}| + \delta_5] \operatorname{sgn}(e_5)\,, \tag{165}$$

$$u_6 = [11(|x_{s6}| + |x_{m6}|) + 12(|x_{s5}| + |x_{m5}|)+ \\ +|\hat{x}_{s2}\hat{x}_{s3}x_{s5}| + |\hat{x}_{m2}\hat{x}_{m3}x_{m5}| + \delta_6] \operatorname{sgn}(e_6)\,, \tag{166}$$

$$u_7 = [7(|x_{s7}| + |x_{m7}|) + 6(|\hat{x}_{s2}| + |\hat{x}_{m2}|)+ \\ +1.5|\hat{x}_{s1}x_{s5}x_{s6}| + 1.5|\hat{x}_{m1}x_{m5}x_{m6}| + \delta_7] \operatorname{sgn}(e_7)\,. \tag{167}$$

Note the message $m(t)$ appears as a perturbation in e_5 dynamics. Thus, by using the equivalent control theory [104], it is possible to recover the message $m(t)$ in receptor side through an approximation by average control. When the system reachs the sliding mode, $\dot{e}_5 = 0$ and $u_5 = u_{eq_5}$, then from (150)

$$\underbrace{-15e_5 + 10e_7 - e_2x_{s3}x_{s4} - x_{m2}e_3x_{s4} - x_{m2}x_{m3}e_4}_{\to 0} - m(t) + u_{eq_5} = 0\,, \tag{168}$$

Although, in theory, the message could be recovered through u_{eq_5}, this signal is not available in practice. Nevertheless, it is possible to find an approximate signal by using the equivalent control theory [104]. According to this theory, an approximation u_{av} for u_{eq} is obtained by filtering the signal u. In our context, the dynamics of u_{av} is given by

$$\tau \dot{u}_{5_{av}}(t) = -u_{5_{av}}(t) + u_5(t)\,, \tag{169}$$

where τ is an appropriate small constant, such that $0 < \tau << 1$. Once in sliding mode, one can state that $u_{5_{av}} \approx u_{5_{eq}}$, then $|u_{5_{av}} - u_{5_{eq}}| \leq \mathscr{O}(\tau) \to 0$. Thus, $u_{5_{av}}(t) \approx u_{5_{eq}}(t) = m(t)$.

In the following simulation results, the parameters are chosen as: $\delta_5 = 3$, $\delta_6 = 0.01$, $\delta_7 = 0.01$. The initial conditions are given by: $x_s(0) = [0.1\,, 0.2\,, 0.3\,, 0.4\,, 0.5\,, 0.6\,, 0.7]^T$, $x_m(0) = [-0.1\,, -0.2\,, -0.3\,, -0.4\,, -0.5\,, -0.6\,, -0.7]^T$ and $\hat{x}_s(0) = \hat{x}_m(0) = [0\,, 0\,, 0\,, 0]^T$.

It can be seen in Figure 23 that the state of the error system (146)–(152) in the synchronization problem is driven to the origin by the output-feedback controller in (165)–(167). Thus, the master (130)–(137) and the slave (138)–(145) oscillators become synchronized.

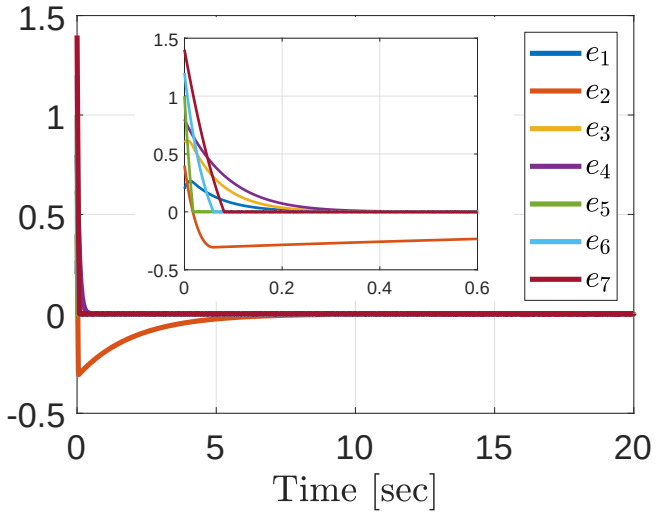

Figure 23: State error signals in the synchronization system.

The message m is incorporated to x_{m_5} dynamics. Hence, it is worth remarking that in the secure communication scheme proposed, the signal m is not directely transmitted to the receptor device. This fact, makes our approach more secure than other possible strategies found in literature [103], [102]. However, when the systems are synchronized, the message can be recovered through extended equivalent control theory. The Figure 24 depicts the recovering process of the message for different τ values. The smaller the τ values, the better is the equivalence between u_{av_5} and u_{eq_5}. Consequently, the better is also the equivalence between u_{av_5} and the original message.

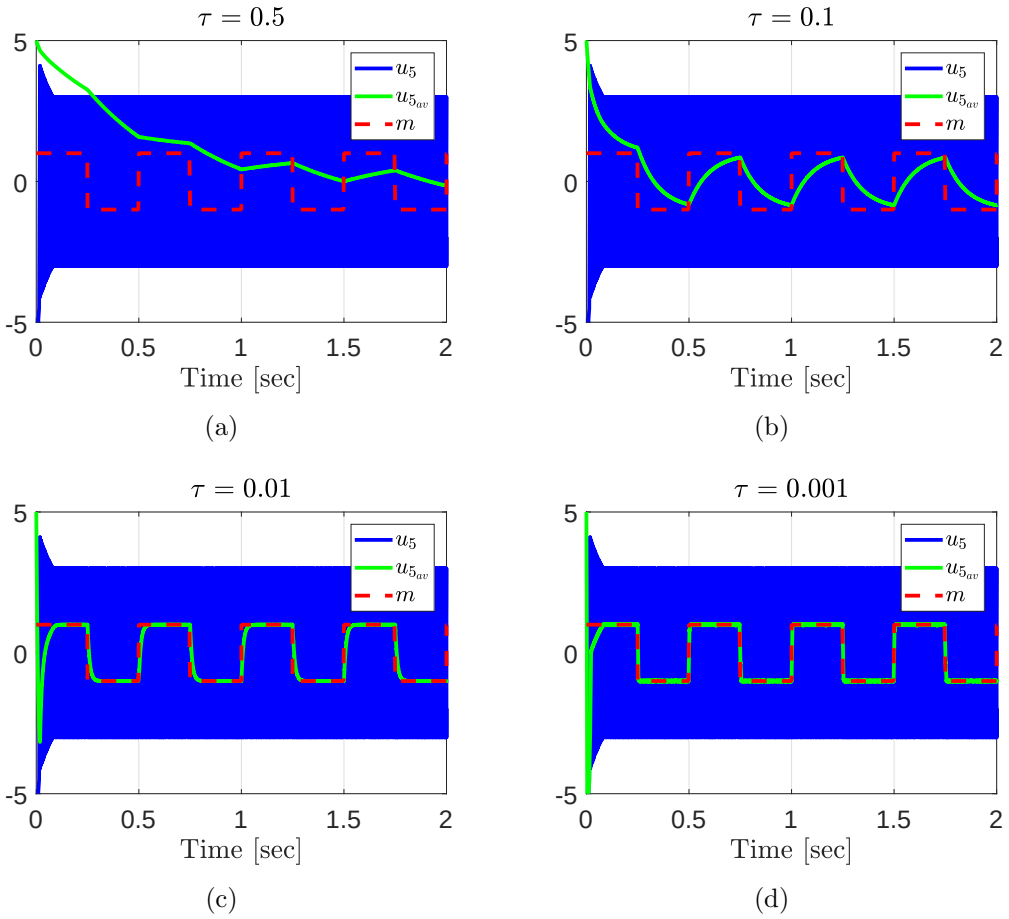

Figure 24: Control signal (u_5), average control (u_{av_5}) and original message (m).

Table 2 presents a class of chaotic systems with ISS properties to which the methodology presented here holds. The cascade norm observers and the control laws demanded in each case are also presented.

Table 2: ISS Chaotic Systems

System	Norm Observers	Control Law
Liu et al., (2004) [96]: $\dot{x}_1 = -10x_1 + 10x_2$ $\dot{x}_2 = 40x_1 - x_1x_3 + u$ $\dot{x}_3 = -2.5x_3 + 4x_1^2$ $y = x_2$	$\dot{\hat{x}}_1 = \bar{\alpha}_1\hat{x}_1 + \bar{\beta}_1\lvert x_2\rvert$ $\dot{\hat{x}}_3 = \bar{\alpha}_3\hat{x}_3 + \bar{\beta}_3\hat{x}_1^2$ $-10 \leq \bar{\alpha}_1 < 0 \quad \bar{\beta}_1 \geq 10$ $-2.5 \leq \bar{\alpha}_3 < 0 \quad \bar{\beta}_3 \geq 4$	$u = -\rho\text{sgn}(y)$ $\rho = \bar{\beta}_2\lvert\hat{x}_1\rvert + \bar{\gamma}_2\lvert\hat{x}_1\hat{x}_3\rvert + \delta$ $\bar{\beta}_2 \geq 40 \quad \bar{\gamma}_2 \geq 1$
Li. et al.,(2010) [108]: $\dot{x}_1 = -12x_1 + 12x_2$ $\dot{x}_2 = 23x_1 - x_1x_3 - x_2 + x_4 + u$ $\dot{x}_3 = x_1x_2 - 2.1x_3$ $\dot{x}_4 = -0.2x_4 - 6x_2$ $y = x_2$	$\dot{\hat{x}}_1 = \bar{\alpha}_1\hat{x}_1 + \bar{\beta}_1\lvert x_2\rvert$ $\dot{\hat{x}}_3 = \bar{\alpha}_3\hat{x}_3 + \bar{\gamma}_3(\hat{x}_1^2 + x_2^2)$ $\dot{\hat{x}}_4 = \bar{\alpha}_4\hat{x}_4 + \bar{\beta}_4\lvert x_2\rvert$ $-12 \leq \bar{\alpha}_1 < 0 \quad \bar{\beta}_1 \geq 12$ $-2.1 \leq \bar{\alpha}_3 < 0 \quad \bar{\gamma}_3 \geq 1$ $-0.2 \leq \bar{\alpha}_4 < 0 \quad \bar{\beta}_4 \geq 6$	$u = -\rho\text{sgn}(y)$ $\rho = \bar{\beta}_2\lvert\hat{x}_1\rvert + \bar{\gamma}_2\lvert\hat{x}_1\hat{x}_3\rvert + \bar{\alpha}_2\lvert x_2\rvert + \bar{\xi}_2\lvert\hat{x}_4\rvert + \delta$ $\bar{\beta}_2 \geq 23 \quad \bar{\gamma}_2 \geq 1$ $\bar{\alpha}_2 \geq 1 \quad \bar{\xi}_2 \geq 1$
Liu et al., (2009) [109]: $\dot{x}_1 = -15x_1 + 15x_2$ $\dot{x}_2 = -x_1x_3 + 10x_2 + x_4 + u$ $\dot{x}_3 = -5x_3 + x_1x_2$ $\dot{x}_4 = -x_4 + x_3$ $y = x_2$	$\dot{\hat{x}}_1 = \bar{\alpha}_1\hat{x}_1 + \bar{\beta}_1\lvert x_2\rvert$ $\dot{\hat{x}}_3 = \bar{\alpha}_3\hat{x}_3 + \bar{\gamma}_3(\hat{x}_1^2 + x_2^2)$ $\dot{\hat{x}}_4 = \bar{\alpha}_4\hat{x}_4 + \bar{\beta}_4\hat{x}_2$ $-15 \leq \bar{\alpha}_1 < 0 \quad \bar{\beta}_1 \geq 15$ $-5 \leq \bar{\alpha}_3 < 0 \quad \bar{\gamma}_3 \geq 1$ $-1 \leq \bar{\alpha}_4 < 0 \quad \bar{\beta}_4 \geq 1$	$u = -\rho\text{sgn}(y)$ $\rho = \bar{\beta}_2\lvert\hat{x}_4\rvert + \bar{\gamma}_2\lvert\hat{x}_1\hat{x}_3\rvert + \bar{\alpha}_2\lvert x_2\rvert + \delta$ $\bar{\alpha}_2 \geq 10 \quad \bar{\beta}_2 \geq 1$ $\bar{\gamma}_2 \geq -1$
Elabbasy et al., (2006) [110]: $\dot{x}_1 = -36x_1 + 36x_2$ $\dot{x}_2 = -x_1x_3 + 20x_2 + u$ $\dot{x}_3 = -3x_3 + x_1x_2$ $y = x_2$	$\dot{\hat{x}}_1 = \bar{\alpha}_1\hat{x}_1 + \bar{\beta}_1\lvert x_2\rvert$ $\dot{\hat{x}}_3 = \bar{\alpha}_3\hat{x}_3 + \bar{\gamma}_3(\hat{x}_1^2 + x_2^2)$ $-36 \leq \bar{\alpha}_1 < 0 \quad \bar{\beta}_1 \geq 36$ $-3 \leq \bar{\alpha}_3 < 0 \quad \bar{\gamma}_3 \geq 1$	$u = -\rho\text{sgn}(y)$ $\rho = \bar{\gamma}_2\lvert\hat{x}_1\hat{x}_3\rvert + \bar{\alpha}_2\lvert x_2\rvert + \delta$ $\bar{\alpha}_2 \geq 1 \quad \bar{\gamma}_2 \geq 20$
Liu et al., (2014) [111]: $\dot{x}_1 = -8x_1 + 8x_2$ $\dot{x}_2 = 40x_1 - 1.5x_1x_3 - 1.2x_4 + u$ $\dot{x}_3 = 1.5x_1x_2 - \frac{10}{3}x_2 - 4x_3$ $\dot{x}_4 = -2x_1 - 2x_4$ $\dot{x}_5 = -2x_3x_4 - 2x_5$ $y = x_2$	$\dot{\hat{x}}_1 = \bar{\alpha}_1\hat{x}_1 + \bar{\beta}_1\lvert x_2\rvert$ $\dot{\hat{x}}_3 = \bar{\alpha}_3\hat{x}_3 + \bar{\beta}_3\lvert x_2\rvert + \bar{\gamma}_3(\hat{x}_1^2 + x_2^2)$ $\dot{\hat{x}}_4 = \bar{\alpha}_4\hat{x}_4 + \bar{\beta}_4\hat{x}_1$ $\dot{\hat{x}}_5 = \bar{\alpha}_5\hat{x}_5 + \bar{\gamma}_5(\hat{x}_3^2 + x_4^2)$ $-8 \leq \bar{\alpha}_1 < 0 \quad \bar{\beta}_1 \geq 8$ $-4 \leq \bar{\alpha}_3 < 0 \;\; \bar{\beta}_3 \geq \frac{10}{3} \quad \bar{\gamma}_3 \geq 1.5$ $-2 \leq \bar{\alpha}_4 < 0 \quad \bar{\beta}_4 \geq 2$ $-2 \leq \bar{\alpha}_5 < 0 \quad \bar{\gamma}_5 \geq 2$	$u = -\rho\text{sgn}(y)$ $\rho = \bar{\beta}_2\lvert\hat{x}_1\rvert + \bar{\gamma}_2\lvert\hat{x}_1\hat{x}_3\rvert + \bar{\xi}_2\lvert\hat{x}_4\rvert + \delta$ $\bar{\beta}_2 \geq 40 \quad \bar{\gamma}_2 \geq 1.5$ $\bar{\xi}_2 \geq 1.2$
Lü and Chen, (2002a) [112]: $\dot{x}_1 = -30x_1 + 30x_2$ $\dot{x}_2 = -x_1x_3 + 22.2x_2 + u$ $\dot{x}_3 = -\frac{8.8}{3}x_3 + x_1x_2$ $y = x_2$	$\dot{\hat{x}}_1 = \bar{\alpha}_1\hat{x}_1 + \bar{\beta}_1\lvert x_2\rvert$ $\dot{\hat{x}}_3 = \bar{\alpha}_3\hat{x}_3 + \bar{\gamma}_3(\hat{x}_1^2 + x_2^2)$ $-30 \leq \bar{\alpha}_1 < 0 \quad \bar{\beta}_1 \geq 30$ $-\frac{8.8}{3} \leq \bar{\alpha}_3 < 0 \quad \bar{\gamma}_3 \geq 1$	$u = -\rho\text{sgn}(y)$ $\rho = \bar{\alpha}_2\lvert x_2\rvert + \bar{\gamma}_2\lvert\hat{x}_1\hat{x}_3\rvert + \delta$ $\bar{\alpha}_2 \geq 22.2 \quad \bar{\gamma}_2 \geq 1$
Lü and Chen, (2002b) [113]: $\dot{x}_1 = (25\phi + 10)(-x_1 + x_2)$ $\dot{x}_2 = (28 - 35\phi)x_1 - x_1x_3 + (29\phi - 1)x_2 + u$ $\dot{x}_3 = -\frac{(8+\phi)}{3}x_3 + x_1x_2$ $y = x_2$	$\dot{\hat{x}}_1 = \bar{\alpha}_1\hat{x}_1 + \bar{\beta}_1\lvert x_2\rvert$ $\dot{\hat{x}}_3 = \bar{\alpha}_3\hat{x}_3 + \bar{\gamma}_3(\hat{x}_1^2 + x_2^2)$ $-\frac{8}{3} \leq \bar{\alpha}_3 < 0 \quad -10 \leq \bar{\alpha}_1 < 0$ $\bar{\gamma}_3 \geq 1 \quad \bar{\beta}_1 \geq 35$	$u = -\rho\text{sgn}(y)$ $\rho = \bar{\beta}_2\lvert\hat{x}_1\rvert + \bar{\alpha}_2\lvert x_2\rvert + \bar{\gamma}_2\lvert\hat{x}_1\hat{x}_3\rvert + \delta$ $\bar{\alpha}_2 \geq 28 \quad \bar{\gamma}_2 \geq 1$ $\bar{\beta}_2 \geq 28$
Chen and Ueta, (1999) [114]: $\dot{x}_1 = -35x_1 + 35x_2$ $\dot{x}_2 = -7x_1 - x_1x_2 + 28x_2 + u$ $\dot{x}_3 = -3x_3 + x_1x_2$ $y = x_2$	$\dot{\hat{x}}_1 = \bar{\alpha}_1\hat{x}_1 + \bar{\beta}_1\lvert x_2\rvert$ $\dot{\hat{x}}_3 = \bar{\alpha}_3\hat{x}_3 + \bar{\gamma}_3(\hat{x}_1^2 + x_2^2)$ $-35 \leq \bar{\alpha}_1 < 0 \quad \bar{\beta}_1 \geq 35$ $-3 \leq \bar{\alpha}_3 < 0 \quad \bar{\gamma}_3 \geq 1$	$u = -\rho\text{sgn}(y)$ $\rho = \bar{\alpha}_2\lvert x_2\rvert + \bar{\gamma}_2\lvert\hat{x}_1\hat{x}_3\rvert + \bar{\beta}_2\lvert\hat{x}_1\rvert + \delta$ $\bar{\alpha}_2 \geq 28 \quad \bar{\beta}_2 \geq 7$ $\bar{\gamma}_2 \geq 1$
Lorenz, (1963) [88]: $\dot{x}_1 = -10x_1 + 10x_2$ $\dot{x}_2 = 28x_1 - x_1x_3 - x_2 + u$ $\dot{x}_3 = -\frac{8}{3}x_3 + x_1x_2$ $y = x_2$	$\dot{\hat{x}}_1 = \bar{\alpha}_1\hat{x}_1 + \bar{\beta}_1\lvert x_2\rvert$ $\dot{\hat{x}}_3 = \bar{\alpha}_3\hat{x}_3 + \bar{\gamma}_3(\hat{x}_1^2 + x_2^2)$ $-10 \leq \bar{\alpha}_1 < 0 \quad \bar{\beta}_1 \geq 10$ $-\frac{8}{3} \leq \bar{\alpha}_3 < 0 \quad \bar{\gamma}_3 \geq 1$	$u = -\rho\text{sgn}(y)$ $\rho = \bar{\alpha}_2\lvert x_2\rvert + \bar{\gamma}_2\lvert\hat{x}_1\hat{x}_3\rvert + \bar{\beta}_2\lvert\hat{x}_1\rvert + \delta$ $\bar{\alpha}_2 \geq 1 \quad \bar{\beta}_2 \geq 28$ $\bar{\gamma}_2 \geq 1$
Liu et al., (2009) [109]: $\dot{x}_1 = -x_1 - x_2^2$ $\dot{x}_2 = 2.5x_2 - 4x_1x_3$ $\dot{x}_3 = -5x_3 + 4x_1x_2$ $y = x_2$	$\dot{\hat{x}}_1 = \bar{\alpha}_1\hat{x}_1 + \bar{\beta}_1x_2^2$ $\dot{\hat{x}}_3 = \bar{\alpha}_3\hat{x}_3 + \bar{\gamma}_3(\hat{x}_1^2 + x_2^2)$ $-1 \leq \bar{\alpha}_1 < 0 \quad \bar{\beta}_1 \geq 1$ $-5 \leq \bar{\alpha}_3 < 0 \quad \bar{\gamma}_3 \geq 4$	$u = -\rho\text{sgn}(y)$ $\rho = \bar{\alpha}_2\lvert x_2\rvert + \bar{\gamma}_2\lvert\hat{x}_1\hat{x}_3\rvert + \delta$ $\bar{\alpha}_2 \geq 2.5 \quad \bar{\gamma}_1 \geq 4$

CONCLUSION

In Chapter 1, two different control strategies based on sliding mode control were used in order to safely regulate the blood glucose concentration of a T1DM patient. From a control point of view, this is a challenging problem since the process is represented by a nonlinear and time-varying model, where the parameters were considered uncertain. Meals of varying carbohydrate content are understood as unmatched disturbances. The output has relative degree two with regard to control signal, and since the model adopted describes a biological process, the control problem must be treated as a strictly positive system.

Such challenges were overcome by using some upper bounds for the plant parameters and disturbances as well as a bihormonal actuator formulation with the sliding mode control theory. A rigorous stability analysis through Lyapunov functions and numerical simulations show that the proposed control strategy was efficient in the glycemic regulation task.

In Chapter 2, exploring the ISS properties from a class of hyperchaotic systems (see Table 2), control laws based on sliding modes and norm observers in cascade can be developed to the stabilization problem. Global stability properties have been demonstrated using only output feedback, even considering that all the parameters of a seventh dimension system were uncertain. Indeed, the proposed controller was shown to be robust to parametric uncertainties and exogenous disturbances.

In addition, the proposed sliding mode controller seems to be an attractive methodology for synchronization, since the convergence of the output signal can be achieved in finite time and the convergence of the other state variables is exponential, being also robust to exogenous disturbances. The application of the synchronization approach to secure communication systems was successfully evaluated. This method provides reliable cryptography using an equivalent control strategy.

As future works, we propose the experimental validation of the presented controllers. Moreover, in an eventual application, we could replace the fixed-gain differentiator presented here by a variable-gain differentiator [115] in order to mitigate the sensitivity of the control system in closed-loop with respect to the measurement error/noise. At last, we suggest the assessment of different sliding mode control techniques aiming to achieve the euglycemia for patients with T1DM.

Publications, Participation in Events and Awards

In the course of my master course that has lead to this dissertation, a plenty of cientific works were published in conferences. Among them,

- DANSA, M. ; RODRIGUES, V. H. P. ; OLIVEIRA, T. R. . Best Paper Presentation in the Session "Epidemic Modeling and Control" of the 22nd International Conference on System Theory, Control and Computing (ICSTCC 2018), IEEE - Institute of Electrical and Electronics Engineers, Sinaia, Romania, October 2018.

- DANSA, M. ; RODRIGUES, V. H. P. ; OLIVEIRA, T. R. . Controlador Bihormonal por Modos Deslizantes Aplicado à Regulação de Glicemia em Pacientes Diabéticos Tipo 1. In: XXII Congresso Brasileiro de Automática (CBA 2018), João Pessoa. Setembro de 2018.

- DANSA, M. ; RODRIGUES, V. H. P. ; OLIVEIRA, T. R. . Bihormonal Sliding Mode Controller Applied to Blood Glucose Regulation in Patients with Type 1 Diabetes. In: 22nd International Conference on System Theory, Control and Computing (ICSTCC 2018), Sinaia. October 2018. p. 79-86.

- DANSA, M. ; RODRIGUES, V. H. P. ; OLIVEIRA, T. R. . Blood Glucose Regulation Through Bihormonal Non-Singular Terminal Sliding Mode Controller. In: 15th International Conference on Control, Automation, Robotics and Vision (ICARCV 2018), Downtown Core. November 2018. p. 474-479.

- DANSA, M. ; RODRIGUES, V. H. P. ; OLIVEIRA, T. R. . Blood Glucose Regulation in Patients with Type 1 Diabetes by means of Output-Feedback Sliding Mode Control. In: Ahmad Taher Azar. (Org.). Control Applications for Biomedical Engineering Systems. XXed.: Elsevier, 2019, p. 1–30.

- DANSA, M. ; RODRIGUES, V. H. P. ; OLIVEIRA, T. R. . Regulação de Glicemia Através de um Controlador Bi-hormonal por Modos Deslizantes Terminal Não-Singular. In: XIV Simpósio Brasileiro de Automação Inteligente (SBAI 2019), Ouro Preto. Outubro de 2019.

REFERENCES

[1] ALBERTOS, P.; MAREELS, I. *Feedback and control for everyone*. [S.l.]: Springer Science & Business Media, 2010.

[2] KRSTIC, M. Feedforward systems linearizable by coordinate change. In: IEEE. *Proceedings of the 2004 American Control Conference*. [S.l.], 2004. v. 5, p. 4348–4353.

[3] TEEL, A. *Feedback Stabilization: Nonlinear Solutions to Inherently Nonlinear Problems*. [S.l.]: University of California, Berkeley, 1992.

[4] TEEL, A. A nonlinear small gain theorem for the analysis of control systems with saturation. *IEEE Transactions on Automatic Control*, IEEE, v. 41, n. 9, p. 1256–1270, 1996.

[5] MAZENC, F.; PRALY, L. Adding integrations, saturated controls, and stabilization for feedforward systems. *IEEE Transactions on Automatic Control*, IEEE, v. 41, n. 11, p. 1559–1578, 1996.

[6] PRALY, L. Adaptive regulation: Lyapunov design with a growth condition. *International Journal of Adaptive Control and Signal Processing*, Wiley Online Library, v. 6, n. 4, p. 329–351, 1992.

[7] PRALY, L. Lyapunov design of a dynamic output feedback for systems linear in their unmeasured state components. In: *Nonlinear Control Systems Design 1992*. [S.l.]: Elsevier, 1993. p. 63–68.

[8] SONTAG, E.; SUSSMANN, H. Nonlinear output feedback design for linear systems with saturating controls. In: IEEE. *29th IEEE Conference on Decision and Control*. [S.l.], 1990. p. 3414–3416.

[9] PRALY, L.; ORTEGA, R.; KALIORA, G. Stabilization of nonlinear systems via forwarding mod {L/sub g/V}. *IEEE Transactions on Automatic Control*, IEEE, v. 46, n. 9, p. 1461–1466, 2001.

[10] JANKOVIC, M.; SEPULCHRE, R.; KOKOTOVIC, P. Constructive Lyapunov stabilization of nonlinear cascade systems. *IEEE Transactions on Automatic Control*, IEEE, v. 41, n. 12, p. 1723–1735, 1996.

[11] SEPULCHRE, R.; JANKOVIC, M.; KOKOTOVIC, P. Integrator forwarding: A new recursive nonlinear robust design. *Automatica*, Elsevier, v. 33, n. 5, p. 979–984, 1997.

[12] ARCAK, M.; TEEL, A.; KOKOTOVIĆ, P. Robust nonlinear control of feedforward systems with unmodeled dynamics. *Automatica*, Elsevier, v. 37, n. 2, p. 265–272, 2001.

[13] MARCONI, L.; ISIDORI, A. Stabilization of nonlinear feedforward systems: A robust approach. In: IEEE. *Proceedings of the 40th IEEE Conference on Decision and Control (Cat. No. 01CH37228)*. [S.l.], 2001. v. 3, p. 2778–2783.

[14] XUDONG, Y. Universal stabilization of feedforward nonlinear systems. *Automatica*, Elsevier, v. 39, n. 1, p. 141–147, 2003.

[15] SEPULCHRE, R.; JANKOVIC, M.; KOKOTOVIC, P. *Constructive Nonlinear Control*. [S.l.]: Springer Science & Business Media, 2012.

[16] MAZENC, F.; SEPULCHRE, R.; JANKOVIC, M. Lyapunov functions for stable cascades and applications to global stabilization. *IEEE Transactions on Automatic Control*, IEEE, v. 44, n. 9, p. 1795–1800, 1999.

[17] MAZENC, F.; PRALY, L. Strict Lyapunov functions for feedforward systems and applications. In: IEEE. *Proceedings of the 39th IEEE Conference on Decision and Control (Cat. No. 00CH37187)*. [S.l.], 2000. v. 4, p. 3875–3880.

[18] TEEL, A. l_2 performance induced by feedbacks with multiple saturations. *ESAIM: Control, Optimisation and Calculus of Variations*, EDP Sciences, v. 1, p. 225–240, 1996.

[19] MAZENC, F.; PRALY, L. Asymptotic tracking of a reference state for systems with a feedforward structure. *Automatica*, Elsevier, v. 36, n. 2, p. 179–187, 2000.

[20] MAZENC, F.; BOWONG, S. Tracking trajectories of feedforward systems. *IEEE Transactions on Automatic Control*, IEEE, v. 47, n. 8, p. 1338–1342, 2002.

[21] MAZENC, F. Stabilization of feedforward systems approximated by a non-linear chain of integrators. *Systems & Control Letters*, Elsevier, v. 32, n. 4, p. 223–229, 1997.

[22] TSINIAS, J.; TZAMTZI, M. An explicit formula of bounded feedback stabilizers for feedforward systems. *Systems & Control Letters*, Elsevier, v. 43, n. 4, p. 247–261, 2001.

[23] GROGNARD, F.; SEPULCHRE, R.; BASTIN, G. Global stabilization of feedforward systems with exponentially unstable jacobian linearization. *Systems & Control Letters*, Elsevier, v. 37, n. 2, p. 107–115, 1999.

[24] MAZENC, F.; NIJMEIJER, H. Forwarding in discrete-time nonlinear systems. *International Journal of Control*, Taylor & Francis, v. 71, n. 5, p. 823–835, 1998.

[25] GROGNARD, F. et al. Nested linear low-gain design for semiglobal stabilization of feedforward systems. *IFAC Nonlinear Control Systems Design*, Koninklijke Vlaamse Ingenieursvereniging, v. 41, n. 2, p. 35–40, 1998.

[26] COLONIUS, F.; GRÜNE, L. *Dynamics, Bifurcations and Control*. [S.l.]: Springer Science & Business Media, 2002.

[27] SPONG, M.; PRALY, L. Control of underactuated mechanical systems using switching and saturation. In: *Control Using Logic-Based Switching*. [S.l.]: Springer, 1997. p. 162–172.

[28] BARBU, C. et al. Global asymptotic stabilization of the ball-and-beam system. In: IEEE. *Proceedings of the 36th IEEE Conference on Decision and Control*. [S.l.], 1997. v. 3, p. 2351–2355.

[29] ALBOUY, X.; PRALY, L. On the use of dynamic invariants and forwarding for swinging up a spherical inverted pendulum. In: *Proceedings of the 39th IEEE Conference on Decision and Control (Cat. No.00CH37187)*. [S.l.: s.n.], 2000. v. 2, p. 1667–1672 vol.2.

[30] MAZENC, F.; BOWONG, S. Tracking trajectories of feedforward systems: Application to the cart-pendulum system. In: IEEE. *Proceedings of the 40th IEEE Conference on Decision and Control (Cat. No. 01CH37228)*. [S.l.], 2001. v. 1, p. 479–484.

[31] PRALY, L. *An introduction to some Lyapunov designs of global asymptotic stabilizers*. Poland, 2-20 September 2002. Lectures notes for the Banach Center Summer School on Mathematical Control Theory.

[32] CORON, J. M.; PRALY, L.; TEEL, A. Feedback stabilization of nonlinear systems: Sufficient conditions and lyapunov and input-output techniques. In: *Trends in control*. [S.l.]: Springer, 1995. p. 293–348.

[33] KOKOTOVIĆ, P.; ARCAK, M. Constructive nonlinear control: A historical perspective. *Automatica*, Elsevier, v. 37, n. 5, p. 637–662, 2001.

[34] EDWARDS, C.; SPURGEON, S. *Sliding Mode Control: Theory and Applications*. [S.l.]: CRC Press, 1998.

[35] UTKIN, V. I. Sliding mode control design principles and applications to electric drives. *Transactions on Industrial Electronics*, IEEE, v. 40, p. 23–36, 1993.

[36] SLOTINE, J. J. E.; LI, W. *Applied nonlinear control*. [S.l.]: Prentice-Hall, 1991.

[37] SLOTINE, J. J.; SASTRY, S. S. Robustness issues in the sliding control of non-linear systems. In: IEEE. *The 22nd IEEE Conference on Decision and Control*. San Antonio, Texas, USA, 1983. p. 1125–1127.

[38] GUYTON, A.; HALL, J. *Textbook of Medical Physiology*. [S.l.]: Elsevier, 2016.

[39] BAKHTIANI, P. et al. A review of artificial pancreas technologies with an emphasis on bi-hormonal therapy. In: *Diabetes, Obesity and Metabolism*. [S.l.]: John Wiley and Sons, 2013. p. 1065–1070.

[40] KADISH, A. Automation control of blood sugar. servomechanism for glucose monitoring and control. *The American journal of medical electronics*, United Technical Publications, v. 9, p. 82–86, 1964.

[41] COBELLI, C.; RENARD, E.; KOVATCHEV, B. Artificial pancreas: Past, present, future. *Diabetes*, American Diabetes Association, v. 60, p. 2672–2682, 2011.

[42] BEQUETTE, B. W. Challenges and recent progress in the development of a closed-loop artificial pancreas. *Annual Reviews in Control*, v. 36, p. 255–266, 2012.

[43] Insulin Pump Awareness Group - IPAG Scotland. *Study: Insulin Pump Better Than Injections*. Disponível em: <https://www.ipag.co.uk/study-insulin-pump-better-than-injections/>. Acesso em: 16 de Abril de 2019.

[44] KAVEH, P.; SHTESSEL, Y. Blood glucose regulation using higher-order sliding mode control. *International Journal of Robust and Nonlinear Control*, Wiley Online Library, v. 18, p. 557–569, 2008.

[45] AUDOLY, S. et al. Global identifiability of nonlinear models of biological systems. *Transactions on Biomedical Engineering*, IEEE, v. 48, p. 55–65, 2001.

[46] HUYETT, L. M. et al. Glucose sensor dynamics and the artificial pancreas: The impact of lag on sensor measurement and controller performance. *IEEE Control Systems Magazine*, IEEE, v. 38, n. 1, p. 30–46, 2018.

[47] MARCHETTI, G. et al. An improved PID switching control strategy for type 1 diabetes. *IEEE Transactions on Biomedical Engineering*, IEEE, v. 55, n. 3, p. 857–865, 2008.

[48] JACOBS, P. et al. Automated control of an adaptive bihormonal, dual-sensor artificial pancreas and evaluation during inpatient studies. *IEEE Transactions on Biomedical Engineering,*, IEEE, v. 61, p. 2569–2581, 2014.

[49] MESSORI, M. et al. Individualized model predictive control for the artificial pancreas: In silico evaluation of closed-loop glucose control. *IEEE Control Systems Magazine*, IEEE, v. 38, n. 1, p. 86–104, 2018.

[50] BÁTORA, V. et al. Bihormonal control of blood glucose in people with type 1 diabetes. In: *2015 European Control Conference (ECC)*. Linz, Austria: [s.n.], 2015. p. 25–30.

[51] BOIROUX, D. et al. Adaptive control in an artificial pancreas for people with type 1 diabetes. *Control Engineering Practice*, Elsevier, v. 58, p. 332–342, 2016.

[52] FAVERO, S. D. et al. Multicenter outpatient dinner/overnight reduction of hypoglycemia and increased time of glucose in target with a wearable artificial pancreas using modular model predictive control in adults with type 1 diabetes. *Diabetes, Obesity and Metabolism*, John Wiley & Sons Ltd., v. 17, n. 5, p. 468476, 2015.

[53] EL-KHATIB, F.; JIANG, B.; DAMIANO, E. Adaptive closed-loop control provides blood-glucose regulation using dual subcutaneous insulin and glucagon infusion in dia-

betic swine. *Journal of Diabetes Science and Technology*, SAGE, v. 1, n. 2, p. 181–192, 2007.

[54] BELLAZZI, R. et al. Adaptive controllers for intelligent monitoring. *Artificial Intelligence in Medicine*, Elsevier, v. 7, n. 6, p. 515–540, 1995.

[55] TURKSOY, K. et al. Multivariable adaptive identification and control for artificial pancreas systems. *IEEE Transactions on Biomedical Engineering*, IEEE, v. 61, n. 3, p. 883–891, 2014.

[56] ATLAS, E. et al. Md-logic artificial pancreas system. *Diabetes Care*, American Diabetes Association, v. 33, p. 1072–1076, 2010.

[57] SHTESSEL, Y.; SHKOLNIKOV, I.; BROWN, M. An asymptotic second-order smooth sliding mode control. *Asian Journal of Control*, John Wiley and Sons, v. 5, p. 498–504, 2003.

[58] JAJARM, A.; OZGOLI, S.; MOMENI, H. Blood glucose regulation using fuzzy recursive fast terminal sliding mode control. In: *4th International Conference on Intelligent and Advanced Systems (ICIAS2012)*. Kuala Lumpur, Malaysia: [s.n.], 2012. p. 393–397.

[59] KUMARESWARAN, K.; EVANS, M.; HOVORKA, R. Artificial pancreas: an emerging approach to treat type 1 diabetes. *Expert Review of Medical Devices*, Taylor & Francis, v. 6, p. 401–410, 2009.

[60] BEQUETTE, B. W. et al. Overnight hypoglycemia and hyperglycemia mitigation for individuals with type 1 diabetes: How risks can be reduced. *IEEE Control Systems Magazine*, IEEE, v. 38, n. 1, p. 125–134, 2018.

[61] EL-KHATIB, F. et al. A bihormonal closed-loop artificial pancreas for type 1 diabetes. *Science Translational Medicine*, American Association for the Advancement of Science, v. 2, p. 27ra27, 2010.

[62] CASTLE, J. et al. Novel use of glucagon in a closed-loop system for prevention of hypoglycemia in type 1 diabetes. *Diabetes Care*, American Diabetes Association, v. 33, p. 1282–1287, 2010.

[63] EL-KHATIB, F. H.; JIANG, J.; DAMIANO, E. R. A feasibility study of bihormonal closed-loop blood glucose control using dual subcutaneous infusion of insulin and glucagon in ambulatory diabetic swine. *Journal of diabetes science and technology*, SAGE Publications, v. 3, p. 789–803, 2009.

[64] BÁTORA, V. et al. Glucagon administration strategies for a dual-hormone artificial pancreas. *IEEE Transactions on Biomedical Engineering*, 2015.

[65] BERGMAN, R.; PHILLIPS, L.; COBELLI, C. Physiologic evaluation of factors controlling glucose tolerance in man – measurement of insulin sensitivity and β–cell glucose sensitivity from the response to intravenous glucose. *Journal of Clinical Investigation*, The American Society for Clinical Investigation, v. 68, p. 1456–1467, 2009.

[66] HERRERO, P. et al. A composite model of glucagon-glucose dynamics for in silico testing of bihormonal glucose controllers. *Journal of Diabetes Science and Technology*, SAGE Publications, v. 7, p. 941–951, 2013.

[67] FARINA, L.; RINALDI, S. *Positive linear systems : theory and applications*. [S.l.]: Wiley, 2000.

[68] BÁTORA, V. et al. The contribution of glucagon in an artificial pancreas for people with type 1 diabetes. In: *2015 American Control Conference*. Chicago, IL, USA: [s.n.], 2015. p. 5097–5102.

[69] RUSSELL, S. et al. Blood glucose control in type 1 diabetes with a bihormonal bionic endocrine pancreas. *Diabetes Care*, American Diabetes Association, v. 35, p. 2148–2155, 2012.

[70] REITER, M.; REITERER, F.; RE, L. del. Bihormonal glucose control using a continuous insulin pump and a glucagon-pen. *European Control Conference (ECC)*, IEEE, p. 2435–2440, 2016.

[71] PATTI, M. New glucagon delivery system reduces episodes of post-bariatric surgery hypoglycemia. *Medical Press*, 2018.

[72] Jonathan Fahey. *How Your Brain Tells Time*. Disponível em: <https://www.forbes.com/2009/10/14/circadian-rhythm-math-technology-breakthroughs-brain.html>. Acesso em: 07 de novembro de 2019.

[73] HANAS, R. *Insulin-dependent Diabetes in Children, Adolescents and Adults - How to become an expert on your own diabetes*. [S.l.]: Class Publishing, 1998.

[74] Abbott Laboratories Ltd. *Abbott FreeStyle Libre User Manual*. Disponível em: <https://www.manualslib.com/manual/1027736/Abbott-Freestyle-Libre.html>. Acesso em: 16 de Abril de 2019.

[75] HERNÁNDEZ, A. et al. High-order sliding-mode control for blood glucose: Practical relative degree approach. *Control Engineering Practice*, Elsevier, v. 21, p. 747–758, 2013.

[76] KHALIL, H. K. *Nonlinear Systems*. [S.l.]: Prentice Hall, 2002.

[77] EDWARDS, C.; SPURGEON, S. K. *Sliding Mode Control: Theory and Applications*. [S.l.]: Taylor & Francis, 1998.

[78] FENG, Y.; YU, X.; MAN, Z. "non-singular terminal sliding mode control of rigid manipulators". *Automatica*, Elsevier, v. 38, p. 2159– 2167, 2002.

[79] FRIDMAN, L.; MORENO, J.; BANDYOPADHYAY, B. *Recent Advances in Sliding Modes: From Control to Intelligent Mechatronics, Editors: X. Yu and M. O. Efe*. [S.l.]: Springer-Verlag, 2015. 5-35 p.

[80] OLIVEIRA, T. R.; ESTRADA, A.; FRIDMAN, L. M. Output-feedback generalization of variable gain super-twisting sliding mode control via global HOSM differentiators. In: IEEE. *14th International Workshop on Variable Structure Systems*. [S.l.], 2016. p. 257–262.

[81] LEVANT, A. Higher-order sliding modes, differentiation and output-feedback control. *International Journal of Control*, Taylor & Francis, v. 76, p. 924–941, 2003.

[82] FRIDMAN, L. et al. Continuous nested algorithms: The fifth generation of sliding mode controllers. In: *Recent advances in sliding modes: from control to intelligent mechatronics*. [S.l.]: Springer, 2015. v. 24, p. 5–36.

[83] GE, S. S.; WANG, C.; LEE, T. H. Adaptive control of chaos in Chua's circuit. *Mathematical Problems in Engineering*, v. 2011, 2011.

[84] MOBAYEN, S. Design of LMI-based global sliding mode controller for uncertain nonlinear systems with application to Genesio's chaotic system. *Complexity*, v. 21, n. 1, p. 94–98, 2014.

[85] PYRAGAS, K. Weak and strong synchronization of chaos. *Physical Review E*, v. 54, n. 5, p. R4508–R4511, 1996.

[86] CUOMO, K. M.; OPPENHEIM, A. V. Circuit implementation of synchronized chaos with applications to communications. *Physical Review Letters*, v. 71, n. 1, p. 65–68, 1993.

[87] HOU, Y.-Y. Controlling chaos in permanent magnet synchronous motor control system via fuzzy guaranteed cost controller. *Mathematical Problems in Engineering*, v. 2012, 2012.

[88] LORENZ, E. N. Deterministic nonperiodic flow. *Journal of the Atmospheric Sciences*, v. 20, p. 130–141, 1963.

[89] SHINBROT, T. et al. Using chaos to direct trajectories to targets. *Physical Review Letters*, v. 65, n. 26, p. 3215–3218, 1990.

[90] IVANCEVIC, T. et al. Nonlinear dynamics and chaos methods in neurodynamics and complex data analysis. *Nonlinear Dynamics*, v. 56, n. 1, p. 23–44, 2008.

[91] JANG, M.-J.; CHEN, C.-L.; CHEN, C.-K. Sliding mode control of chaos in the cubic Chua's circuit system. *International Journal of Bifurcation and Chaos*, v. 12, p. 1437–1449, 2002.

[92] NAZZAL, J. M.; NATSHEH, A. N. Chaos control using sliding–mode theory. *Chaos, Solitons and Fractals*, v. 33, p. 695–702, 2007.

[93] CHUA, L. O. The genesis of Chua's circuit. *Archiv fur Elektronik und Ubertragungstechnik*, v. 46, p. 250–257, 1992.

[94] WANG, C.; GE, S. S. Adaptive backstepping control of uncertain Lorenz system. *International Journal of Bifurcation and Chaos*, v. 11, p. 1115–1119, 2001.

[95] ARAUJO, A. D.; SINGH, S. N. Output-feedback adaptive variable structure control of chaos in Lorenz system. *International Journal of Bifurcation and Chaos*, v. 12, n. 03, p. 571–582, 2002.

[96] LIU, C. et al. A new chaotic attractor. *Chaos, Solitons and Fractals*, v. 22, p. 1031–1038, 2004.

[97] DADRAS, S.; MOMENI, H. R.; MAJD, V. J. Sliding mode control for uncertain new chaotic dynamical system. *Chaos, Solitons and Fractals*, v. 41, p. 1857–1862, 2009.

[98] EL-KHAZALI, R.; AHMAD, W.; AL-ASSAF, Y. Sliding mode control of generalized fractional chaotic systems. *International Journal of Bifurcation and Chaos*, v. 16, n. 10, p. 3113–3125, 2006.

[99] LIU, L.; HAN, Z.; LI, W. Global sliding mode control and application in chaotic systems. *Nonlinear Dynamics*, v. 56, n. 1, p. 193–198, 2008.

[100] LIU, L. et al. Hyperchaos synchronization of fractional-order arbitrary dimensional dynamical systems via modified sliding mode control. *Nonlinear Dynamics*, v. 76, n. 4, p. 20592071, 2014.

[101] RODRIGUES, V. P.; OLIVEIRA, T.; CUNHA, J. P. Globally stable synchronization of chaotic systems based on norm observers connected in cascade. *IEEE Transactions on Circuits and Systems II: Express Briefs*, v. 63, n. 9, p. 883–887, 2016.

[102] PERRUQUETTI, W.; FLOQUET, T.; MOULAY, E. Finite-time observers: Application to secure communication. *IEEE Transactions on Automatic Control*, v. 53, n. 1, p. 356–360, 2008.

[103] JIANG, Z. A note on chaotic secure communication systems. *IEEE Transactions on Circuits and Systems I Fundamental Theory and Applications*, v. 49, n. 1, p. 92–96, 2002.

[104] UTKIN, V. I. *Sliding Modes and Their Application in Variable Structure Systems.* [S.l.]: Mir Publishers, 1978.

[105] LIU, D.; ZHU, J.; SUN, H. Seven-dimensional third-order hyperchaotic system and it's applications in image encryption. *Advanced Science and Technology Letters*, v. 31, p. 119–125, 2013.

[106] FILIPPOV, A. F. *Differential Equations with Discontinuous Right-Hand Side*. [S.l.]: American Mathematical Society Translations, 1964.

[107] RODRIGUES, V. H. P.; DANSA, M. M.; OLIVEIRA, T. R. Estabilização global para uma classe de sistemas hipercaóticos através de observadores da norma em cascata. XII Simpósio Brasileiro de Automação Inteligente, 2015.

[108] LI., Y. et al. A new hyperchaotic Lorenz-type system: Generation, analysis, and implementation. *International Journal of Circuit Theory and Applications*, v. 39, p. 865–879, 2010.

[109] LIU, C.; LIU, L.; LIU, T. A novel three-dimensional autonomous chaos system. *Chaos, Solitons and Fractals*, v. 39, p. 1950–1958, 2009.

[110] ELABBASY, E. M.; AGIZA, H. N.; EL-DESSOKY, M. M. Adaptive synchronization of a hyperchaotic system with uncertain parameter. *Chaos, Solitons and Fractals*, v. 30, p. 1133–1142, 2006.

[111] LIU, L. et al. Hyperchaos synchronization of fractional-order arbitrary dimensional dynamical systems via modified sliding mode control. *Chaos, Solitons and Fractals*, v. 22, p. 2059–2071, 2014.

[112] LÜ, J. H.; CHEN, G. R. New chaotic attractor coined. *International Journal of Bifurcation and Chaos*, v. 12, p. 659–661, 2002.

[113] LÜ, J. H.; CHEN, G. R. Bridge the gap between the Lorenz system and the Chen system. *International Journal of Bifurcation and Chaos*, v. 12, p. 2917–2926, 2002.

[114] CHEN, G.; UETA, T. Yet another chaotic attractor. *International Journal of Bifurcation and Chaos*, v. 09, n. 07, p. 1465–1466, 1999.

[115] OLIVEIRA, T. R.; ESTRADA, A.; FRIDMAN, L. M. Global and exact hosm differentiator with dynamic gains for output-feedback sliding mode control. *Automatica*, v. 81, p. 156–163, 2017.